On the viability of catalytic turnover via Al-O/B-H metathesis: the reactivity of β-diketiminate aluminium hydrides towards CO_2 and boranes

Alexa Caise,[a] Dafydd Jones,[a] Eugene L. Kolychev,[a] Jamie Hicks,[a] Jose M. Goicoechea[a] and Simon Aldridge[a]*

Abstract: A series of novel β-diketiminate stabilized aluminium hydrides of the type (Nacnac)Al(R)H has been synthesized offering variation in the auxiliary R substituent and in the Nacnac backbone itself. These show significant variation in the nature of the Al-H bond (as revealed by widely differing IR stretching frequencies) and marked differences in reactivity with respect to the insertion of CO_2. Electron-donating R groups give rise to weaker (and presumably more hydridic) Al-H bonds, leading to enhanced rates of reactivity towards CO_2. The resulting κ^1-formate complexes (Nacnac)Al(R){OC(O)H} have been isolated and their reactivity towards B-H containing reductants probed. In the case of HBpin no reaction is observed (even under forcing conditions), while the more reactive boranes HBcat and $\{H(9\text{-BBN})\}_2$ ultimately yield boryloxy complexes of the type (Nacnac)Al(R)(OBX_2) (X_2 = cat, 9-BBN). However, no hint of Al-O/B-H metathesis is observed even under forcing conditions. With $BH_3{\cdot}SMe_2$ the major product is a related boryloxy system, although (uniquely) in this case a minor product is observed which contains an Al-H bond. We hypothesize that (Nacnac)Al(R)(κ^2-BH_4) is formed (despite the unfavourable thermodynamics of Al-O/B-H metathesis) due to the additional driving force provided by coordination of the strongly Lewis acidic BH_3 unit to the Al-H bond. That said, we find that (unlike with the analogous gallium systems) no catalytic turnover is achieved in the reduction of CO_2 by boranes mediated by these aluminium hydrides.

Introduction

In the burgeoning field of small molecule activation, the reduction of CO_2 has recently received appreciable attention, not least because it can produce compounds such as methanol, carbon monoxide and formaldehyde which are useful C_1 synthetic building blocks.[1-5] The use of metal hydrides is one approach used to mediate the catalytic reduction of CO_2, and systems incorporating both transition metal and main group elements have been shown to be effective catalysts.[6-14] Generally, the activation of CO_2 occurs by insertion into the M-H bond, followed by liberation of the derived formate moiety from the metal centre and regeneration of the metal hydride catalyst, by employing a reductant such as a borane or silane.[15] Examples of main group metal hydrides that function as catalysts for this process include derivatives of inexpensive alkaline earth metals, group 13 and 14 elements.[16-24]

In 2015, we reported a gallium(III) hydride, [^{Dipp}**1**]Ga(^{t}Bu)H ([^{Dipp}**1**] = HC(MeCDippN)$_2$), that selectively catalyses the reduction of CO_2 to either methanol or formic acid equivalents when employed in conjunction with HBpin, albeit with relatively low turnover frequencies.[23] The two steps critical to turnover in this catalytic process - insertion of CO_2 into the Ga-H bond and metathesis with HBpin to generate a formate ester, could be independently verified via stoichiometric reactions. The extension of this chemistry to aluminium hydrides is little explored, despite potential benefits from both cost and chemical perspectives. Aluminium is much less expensive/more abundant than its heavier congener, and the greater polarity of Al-H bonds might be expected to render them more amenable to rapid insertion of CO_2.[25]

Examples of the *stoichiometric* hydroalumination of CO_2 by molecular aluminium hydrides have been reported, and the use of $LiAlH_4$ to reduce carbon dioxide dates back to the 1950s.[26-28] Moreover, from a catalysis perspective, aluminium hydrides have been implicated as catalysts in a range of reactions of other unsaturated substrates. Several systems, for example, are capable of bringing about the catalytic hydroboration of alkenes and alkynes.[29-32] Additionally, the cationic aluminium hydride complex [(^{Dipp}**1**)AlH][BAr^f_4] functions as a hydrosilylation catalyst, although this chemistry is proposed to proceed by Lewis acid activation of substrate(s), rather than via insertion into the Al-H bond.[33] Most interesting to us, however (given our interests in oxygen-containing substrates) are a number of recent reports detailing the use of aluminium hydrides in the catalytic hydroboration of aldehydes and ketones (Figure 1).[32,34-36]

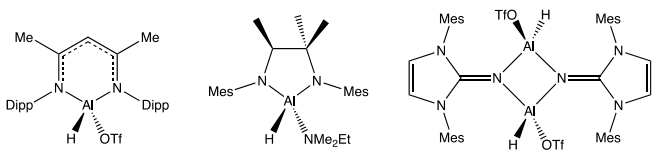

Figure 1. Selected examples of aluminium hydrides which catalyse the hydroboration of aldehydes and ketones with HBpin at room temperature.

[a] Ms Alexa Caise, Mr Dafydd Jones, Dr Eugene L. Kolychev, Dr Jamie Hicks, Prof Jose M. Goicoechea,* Prof Simon Aldridge*
Inorganic Chemistry Laboratory
Department of Chemistry
University of Oxford
South Parks Road
Oxford, OX1 3QR, UK
E-mail: simon.aldridge@chem.ox.ac.uk,
jose.goicoechea@chem.ox.ac.uk

Supporting information for this article is given via a link at the end of the document.

These systems are proposed to turn over by initial hydroalumination of the C=O functionality to yield an aluminium alkoxide, followed by reaction with HBpin (via Al-O/B-H σ-bond metathesis) to regenerate the active Al-H bond.[34] This mechanism is superficially similar to that reported for the [^{Dipp}**1**]Ga(^{t}Bu)H catalysed reduction of CO_2 (Scheme 1)[23] and this, together with the known capabilities of aluminium hydrides in the stoichiometric hydroalumination of CO_2, suggested to us that they might be capable of functioning as catalysts for this process. To the best of our knowledge the catalytic reduction of CO_2 mediated by an aluminium hydride has not been reported.[37]

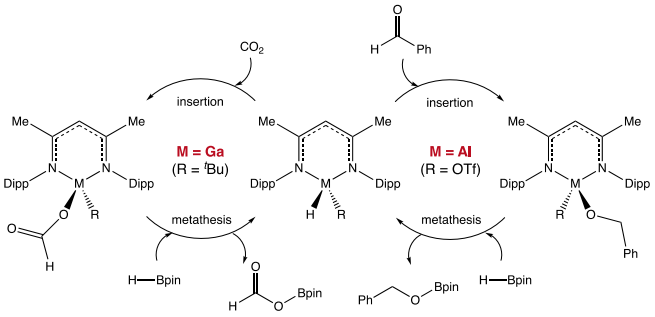

Scheme 1. Reported catalytic cycles for the catalytic reduction of CO_2 (left) and benzaldehyde (right), catalysed by Nacnac-ligated group 13 monohydrides.[23,34]

With this in mind, we set out to investigate the chemistry of a range of well-defiined β-diketiminate-stabilized aluminium hydrides in the presence of CO_2 and various boranes. Our intention at the outset was to probe the viability of the key insertion and metathesis steps as a function of the aluminium hydride and borane reductant. We report on these studies in this publication, which examines sequentially (i) the synthesis of a range of β-diketiminate stabilized aluminium hydrides; (ii) insertion of CO_2 into Al-H bonds, with the aim of identifying structure/activity relationships; and (iii) the possibility for regeneration of the Al-H bond by Al-O/B-H metathesis using borane reductants.

Results and Discussion

Syntheses of novel β-diketiminato aluminium hydrides

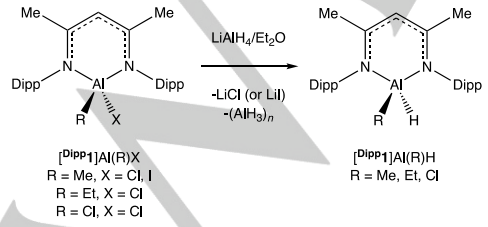

Scheme 2. Synthesis of novel aluminium hydride complexes [^{Dipp}**1**]Al(R)H (R = Me, Et, Cl).

Treatment of the aluminium halide complexes [^{Dipp}**1**]Al(R)Cl (R = Me, Et, Cl) or [^{Dipp}**1**]Al(Me)I with one equivalent of $LiAlH_4$ at −78°C cleanly yields the Nacnac-ligated aluminium hydride complexes [^{Dipp}**1**]Al(R)H in high yields (R = Me: 65%; R = Et: 79%; R = Cl 77%; Scheme 2). Each has been characterised by standard spectroscopic and analytical techniques, and their molecular structures determined by X-ray crystallography (Figure 2). Common features observed in the respective ^{1}H NMR spectra include four doublets for the Dipp methyl groups and two septets for the Dipp methine groups, consistent with an unsymmetrical substitution pattern at aluminium. The ^{27}Al NMR resonances are characteristic of four-coordinate aluminium environments (e.g. δ_{Al} = 143 ppm for [^{Dipp}**1**]Al(Me)H), and the aluminium-bound hydrogens give rise to quadrupolar-broadened ^{1}H NMR resonances at chemical shifts typical of aluminium hydrides (e.g. δ_H = 4.64 ppm for [^{Dipp}**1**]Al(Me)H).[25] In the case of [^{Dipp}**1**]Al(Me)H, the Al-CH_3 resonance (at δ_H = −0.74 ppm) is shifted considerably upfield relative to that of its chloride precursor [^{Dipp}**1**]Al(Me)Cl (δ_H −0.31 ppm), reflecting the increase in shielding arising from the highly σ-donating character of the aluminium-bound hydride. Crystallographic studies of these hydrides reveal that they are monomeric in the solid state, consistent with the previously reported Nacnac-ligated alanes, in which both the coordinatively saturated nature of the metal centre, and the high degree of steric protection provided by the ligand inhibit oligomerisation.[38]

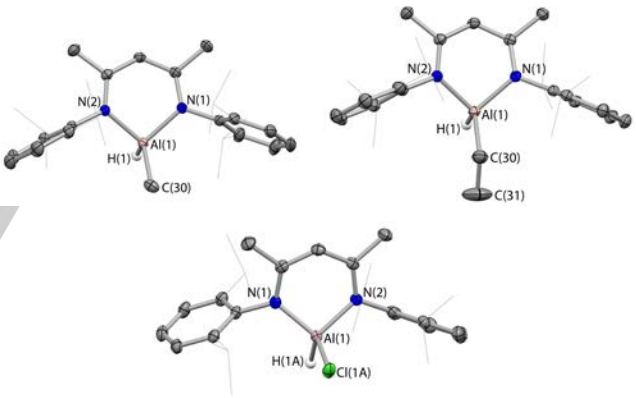

Figure 2. Molecular structures of [^{Dipp}**1**]Al(Me)H (top left), [^{Dipp}**1**]Al(Et)H (top right) and [^{Dipp}**1**]Al(Cl)H (bottom) as determined by X-ray crysytallography. Thermal ellipsoids set at the 40% probability level. Selected H atoms and second disorder component for [^{Dipp}**1**]Al(Cl)H omitted, and Dipp groups shown in wireframe for clarity. Al-Hs located in the difference Fourier map and refined isotropically. Key bond lengths (Å) and angles (°) are listed in Table 1.

□□ la□□□ complexes featuring the electronically modified N-nacnac ligand can also be accessed readily,[39] either directly from the protio ligand, or via metathesis chemistry analogous to that outlined in Scheme 2. Thus, addition of [^{Dipp}**2**]H ([^{Dipp}**2**] = HC{(Me_2N)CDippN}$_2$) to a solution of $Me_3N{\cdot}AlH_3$ in toluene at 0°C yields the dihydride [^{Dipp}**2**]AlH_2 in 64% yield (Scheme 3). Crystalline samples could be obtained from hexane at −30°C, and [^{Dipp}**2**]AlH_2 was fully characterised by standard spectroscopic and analytical techniques, in addition to X-ray crystallography (Figure 3).

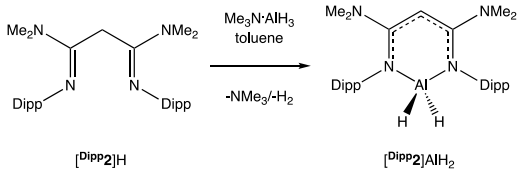

Scheme 3. Synthesis of [Dipp**2**]AlH_2 from the *protio*-ligand [Dipp**2**]H and $Me_3N{\cdot}AlH_3$.

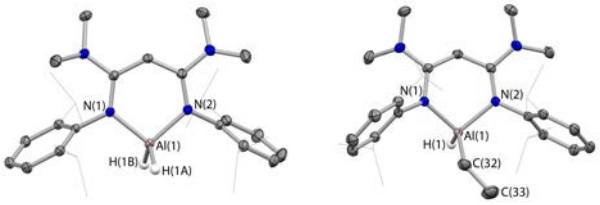

Figure 3. Molecular structures of one of the components of the asymmetric unit of [Dipp**2**]AlH_2 (left) and [Dipp**2**]Al(Et)H (right) as determined by X-ray crystallography. Thermal ellipsoids set at the 40% probability level. Selected hydrogen atoms omitted and Dipp groups shown in wireframe for clarity. Al-H located in the Fourier difference map and refined isotropically. Key bond lengths (Å) and angles (°): (for [Dipp**2**]AlH_2): Al(1)-N(1) 1.892(1), Al(1)-N(2) 1.894(1), Al(1)-H(1A) 1.47(2), Al(1)-H(1B) 1.55(2), N(1)-Al(1)-N(2) 100.6(1); (for [Dipp**2**]Al(Et)H): Al(1)-N(1) 1.895(1), Al(1)-N(2) 1.922(1), Al(1)-C(32) 1.980(1), Al(1)-H(1) 1.52(2), N(1)-Al(1)-N(2) 99.4(1).

The ^{1}H NMR spectrum of [Dipp**2**]AlH_2 features a single septet and two doublets in the aliphatic region, corresponding to the Dipp isopropyl groups of a symmetrical product (i.e. one possessing C_{2v} symmetry). The spectrum also contains a broad signal at δ_H = 4.52 ppm corresponding to the two aluminium-bound hydrogens. As is reported for other systems of this type, the resonance that corresponds to the N-nacnac backbone C-H (at δ_H = 3.84 ppm) is considerably more upfield than that of its 'regular' Nacnac analogue [Dipp**1**]AlH_2 (δ_H = 4.86 ppm), a phenomenon thought to arise from π-electron delocalisation from the NMe_2 groups into the ligand backbone.[39]

Metathesis can also be employed to generate unsymmetrically substituted N-nacnac complexes. Thus, addition of a slight excess of $LiAlH_4$ to an ethereal solution of the mixed ethyl/chloro system [Dipp**2**]Al(Et)Cl at −78°C yields [Dipp**2**]Al(Et)H in 52% yield (Scheme 4). [Dipp**2**]Al(Et)H was also characterised by standard spectroscopic and analytical techniques, and its molecular structure elucidated by X-ray crystallography (Figure 3). Key ^{1}H NMR signals for [Dipp**2**]Al(Et)H are found at at δ_H = 4.90 ppm (Al-H) and δ_H = 3.67 ppm (N-nacnac backbone C-H), the latter showing the expected upfield shift compared to that of [Dipp**1**]Al(Et)H (δ_H = 4.92 ppm).

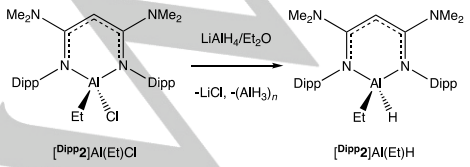

Scheme 4. Synthesis of [Dipp**2**]Al(Et)H via Cl/H metathesis

Trends in crystallographic and IR data

Each of the new Nacnac hydrides, [Dipp**1**]Al(R)H (R = Me, Et, Cl), features a distorted tetrahedral aluminium centre which is projected out of the plane of the Nacnac ligand (Figure 4 and Table 1). The deviation of the six-membered C_3N_2Al heterocycle from planarity is smaller for these hydride derivatives, relative to their chloride precursors. Folding of the ring reduces sterically unfavourable interactions between the Dipp and metal-bound substituents. Increased planarity is therefore associated with smaller substituents, such as hydrides.[40] Consistently, greater distortion is observed on increasing the size of the R substituent from hydride to chloride to ethyl. This effect is also accompanied by a marked narrowing of the N-Al-N angle as the aluminium centre is displaced further from the C_3N_2 plane.

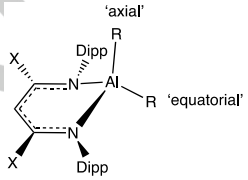

Figure 4. 'Axial' and 'equatorial' substituents in non-planar aluminium Nacnac derivatives.

Table 1: Comparison of key structural parameters of β-diketiminate aluminium hydrides.[40-42]

Parameter[a]	Distance of Al from C_3N_2 plane	*d*(Al-N)	*d*(Al-R)	*d*(Al-H)	N-Al-N angle
[Dipp**1**]Al(Me)H	0.614	1.908(1) 1.912(1)	2.000(2)	1.58(1)	96.1(1)
[Dipp**1**]Al(Me)Cl	0.664	1.906(2) 1.887(2)	1.905(5)	-	97.6(1)
[Dipp**1**]Al(Et)H	0.663	1.915(1) 1.917(1)	1.960(2)	1.67(4)	95.1(1)
[Dipp**1**]Al(Et)Cl	0.693	1.898(1) 1.884(1)	1.955(2)	-	96.9(1)
[Dipp**2**]Al(Et)H	0.464	1.895(1) 1.922(1)	1.980(1)	1.52(2)	99.4(1)
[Dipp**2**]Al(Et)Cl	0.667	1.891(1) 1.887(1)	1.971(1)	-	101.7(1)
[Dipp**1**]Al(Cl)H	0.467	1.875(1) 1.890(1)	2.137(1)	1.55(3)	98.5(1)
[Dipp**1**]$AlCl_2$	0.525	1.884(1) 1.866(1)	2.119(1) 2.134(1)	-	99.4(1)
[Dipp**1**]AlH_2	0.006	1.899(1)	-	1.51(2) 1.52(2)	96.4(1)
[Dipp**2**]AlH_2[b]	0.016 0.095	1.892(1) 1.894(1) 1.890(1) 1.896(1)	-	1.47(2) 1.55(2) 1.52(2) 1.54(2)	100.6(1) 100.1(1)

The non-planar C_3N_2Al skeleton renders the sites occupied by the two aluminium-bound substituents inequivalent, resulting in distinct 'axial' and 'equatorial' positions (Figure 4). Typically, the larger substituent occupies the less sterically hindered 'equatorial' position. Thus, in the solid-state structures of [Dipp**1**]Al(R)H (R = Me, Et) the alkyl substituents are equatorial,

while in [^{Dipp}**1**]Al(Cl)H, the chloride and hydride substituents are disordered across both positions, implying a smaller difference in the size of the two substituents. This structural feature is also observed for [**Dipp1**]Al(Me)Cl.[41] From the perspective of bond metrics, the replacement of the electronegative chloride substituent in the precursor systems with a σ-donating hydride group, results in the lengthening of the remaining bonds to the aluminium centre, presumably reflecting a reduction in its Lewis acidity. Thus, for example the Al-N distances for [**Dipp1**]Al(Et)Cl and [**Dipp1**]Al(Et)H are 1.898(1)/1.884(1) and 1.915(1)/1.917(1) Å, respectively. In all cases, the hydride ligand(s) could be located in the difference Fourier map and were refined isotropically; the Al-H distances are consistent with literature precedent.[40,43]

Crystallographic characterization of the N-nacnac derivatives [**Dipp2**]AlH_2 and [**Dipp2**]Al(Et)H reveals structural features which are in line with their 'regular' Nacnac-ligated counterparts. Thus, the aluminium centre in [**Dipp2**]AlH_2 lies only marginally (0.046 Å, mean) out of the least-squares C_3N_2 plane, as is also found with [**Dipp1**]AlH_2.[40] Ethyl/hydride complexes [**Dipp1**]Al(Et)H and [**Dipp2**]Al(Et)H feature only minimal differences in the Al-N and Al-C distances, although the metal lies noticeably closer to the least-squares C_3N_2 plane in the N-nacnac compound (0.464 *vs.* 0.663 Å) and, as a result, widening of the N-Al-N angle is observed (99.4(1)° vs. 95.1(1)°). The apparently small structural influence of the backbone amino groups presumably reflects – at least in part – the fact that the (planar) NMe_2 functions do not lie coplanar with the C_3N_2Al ring. The torsion angles between the respective planes in [**Dipp2**]AlH_2 are 31.8 and 34.2°.[39]

While Al-H bond metrics are not easily established from X-ray crystallography, the stretching frequencies measured by IR for the hydride derivatives do provide a potentially informative probe of the nature of the Al-H bond. Such data is potentially useful in establishing structure/activity relationships, given the likely influence of the Al-H bond strength/polarity on the rate of insertion of CO_2. In the case of [**Dipp1**]Al(Cl)H two Al-H stretching bands are observed at 1865 cm^{-1} and 1842 cm^{-1}, arising from the disordered nature of the Cl and H substituents in the axial/equatorial positions in the solid state. These data are comparable to those measured for related species bearing electron-withdrawing groups (*e.g.* 1854, 1824 cm^{-1} for R = NHPh, O^{i}Pr). By contrast, the Al-H stretches measured for [**Dipp1**]Al(Me)H (1767 cm^{-1}) and [**Dipp1**]Al(Et)H (1776 cm^{-1}) are considerably red-shifted, and represent some of the lowest Al-H stretching frequencies measured for complexes of this type.[43] The influence of the Nacnac backbone substituents is much less pronounced: the mean Al-H stretching frequency measured for [**Dipp2**]AlH_2 (1817 cm^{-1}) is essentially identical to that of [**Dipp1**]AlH_2 (1814 cm^{-1}), and that measured for [**Dipp2**]Al(Et)H (1788 cm^{-1}) is marginally (12 cm^{-1}) higher than that of its 'regular' Nacnac analogue.

A degree of correlation of the Al-H stretching frequency with the electronic character of the aluminium-bound substituent is apparent:[43,48] in particular, the presence of electron-withdrawing substituents leads to blue-shifted stretching frequencies. Such substituents presumably bring about a lowering in energy of aluminium-centred orbitals and more effective overlap with those of the hydrogen atom, leading to a stronger bond and a higher stretching frequency.[44]

Reactivity of β-diketiminate ligated aluminium hydrides towards CO_2

There are a number of examples of aluminium hydrides which react with CO_2, in which one of the C=O bonds inserts into the Al-H bond to yield an aluminium formate.[26-28] However, while a range of well-defined Nacnac-ligated aluminium hydrides is available, the reaction chemistry of these systems towards CO_2 has not been reported. With this in mind, the reactivity of our new systems (and related alanes) towards CO_2 was targeted with the aims of (i) defining potential modes of reactivity; and (ii) understanding the factors controlling the relative rates of reaction. In the event, systems could be divided into three distinct cases: those inert to CO_2 insertion; compounds undergoing insertion into one Al-H bond to give a formate; and those undergoing insertion into two bonds to give an acetal derivative.

Initial scoping of reactivity focussed on [**Dipp1**]Al(Cl)H and the related triflate system [**Dipp1**]Al(OTf)H, reported recently by Roesky and co-workers.[34] However, monitoring by ^{1}H NMR spectroscopy revealed that no reaction occurs with either of these compounds at room temperature/1 atm. CO_2 or on heating the reaction mixture to 80°C for several days (Scheme 5).

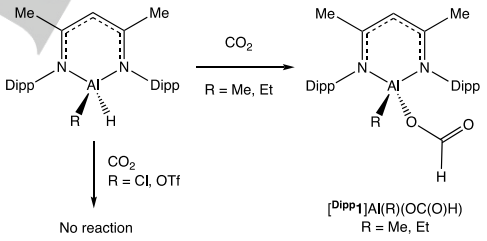

Scheme 5. Reactivity of [**Dipp1**]Al(R)H (R = Cl, OTf, Me, Et) towards CO_2.

By contrast, solutions of the alkylaluminium hydrides [**Dipp1**]Al(Me)H and [**Dipp1**]Al(Et)H react readily under ambient pressures of CO_2 at room temperature to selectively yield the respective formate complexes [**Dipp1**]Al(R){OC(O)H)} (R = Me, Et). The insertion of CO_2 in each case is signalled by the loss of the Al-H ^{1}H NMR resonance and the appearance of a sharp downfield resonance diagnostic of the formate function (at δ_H = 8.46 and 8.49 ppm, respectively). Downfield $^{13}C\{^1H\}$ NMR resonances at δ_C = 162.4 and 162.7 ppm also support the formation of the formate ligand.[23] In addition, the IR spectra each feature a strong band (at 1673 cm^{-1} and 1680 cm^{-1}, respectively) in the region characteristic of the formate C=O stretching mode.[23]

^{1}H NMR spectroscopy reveals these transformations to be quantitative, and although there is literature precedent for insertion of CO_2 into aluminium-alkyl bonds, this is not evident in these systems.[45] [**Dipp1**]Al(R){OC(O)H} (R = Me, Et) can be isolated in yields of 65% and 90% respectively, following

recrystallization from *n*-hexane. Both complexes have been characterised by standard analytical and spectroscopic techniques, in addition to X-ray crystallography (Figure 5). These systems represent rare structurally characterised aluminium formate complexes in which the formate ligand acts as a monodentate κ^1 ligand. The molecular structures feature two distinct C-O bond lengths, consistent with single and double C-O bonds, and a trigonal planar environment around the formate carbon.[23,26]

In order to quantify the respective rates of CO_2 insertion into [**Dipp1**]Al(Me)H and [**Dipp1**]Al(Et)H, solutions of both compounds in benzene-d_6 were placed under 1 bar of CO_2 and the formation of the formate monitored by ^{1}H NMR spectroscopy (ESI). The reaction reaches > 90% completion after *ca*. 40 min for [**Dipp1**]Al(Me)H and 60 min for [**Dipp1**]Al(Et)H. Both reactions show first order kinetics and comparable rate constants (7.16×10^{-4} s^{-1} and 6.16×10^{-4} s^{-1}, respectively). Single-site mechanisms for CO_2 reduction have been postulated computationally to involve initial nucleophilic attack of a metal hydride at the C-centre of CO_2,[46] and, as such, the nature of the M-H bond would be expected to plays significant role in determining the rate of reaction. The differences in the rates of reactivity of these aluminium hydrides compared to [^{Dipp}**1**]Ga(^{t}Bu)H (which takes > 12 h to go to completion) are consistent with this idea, given that Al-H bonds are known to be significantly more hydridic than their gallium counterparts. Similar factors presumably underpin the effect of the second aluminium-bound substituent, R. The presence of an electron-withdrawing R substituent - such as Cl or OTf - reduces the hydridic character of the Al-H bond and consequently its reactivity towards CO_2: unlike their alkyl-substituted counterparts, [**Dipp1**]Al(Cl)H and [**Dipp1**]Al(OTf)H are unreactive towards CO_2. This behaviour also correlates well with the measured Al-H stretching frequencies, (1854 cm^{-1} (mean)/1905 cm^{-1} for R = Cl/OTf and 1767/1776 cm^{-1} for R = Me/Et), with the stronger bonds proving unreactive towards CO_2.

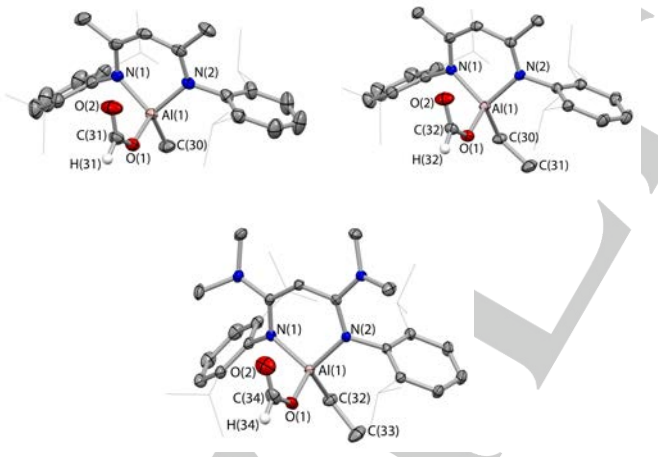

Figure 5. Molecular structures of [**Dipp1**]Al(Me){OC(O)H} (top left), [**Dipp1**]Al(Et){OC(O)H} (top right) and [^{Dipp}**2**]Al(Et){OC(O)H} (bottom) as determined by X-ray crystallography. Thermal ellipsoids set at the 40% probability level. Selected hydrogen atoms and solvate molecule for [**Dipp1**]Al(Et){OC(O)H} omitted, and Dipp groups shown in wireframe for clarity. Key bond lengths (Å) and angles (°): (for [**Dipp1**]Al(Me){OC(O)H}): Al(1)-O(1) 1.780(3), Al(1)-N(1) 1.891(2), Al(1)-N(2) 1.890(3), Al(1)-C(30) 1.937(4), O(1)-C(31) 1.295(4), O(2)-C(31) 1.205(5), N(5)-Al(1)-N(9) 97.2(1); (for [**Dipp1**]Al(Et){OC(O)H}): Al(1)-O(1) 1.786(1), Al(1)-N(1) 1.885(1), Al(1)-N(2) 1.892(1), Al(1)-C(30) 1.958(1), O(1)-C(32) 1.305(2), O(2)-C(32) 1.202(2), N(1)-Al(1)-N(2) 97.5(1); (for [^{Dipp}**2**]Al(Et){OC(O)H}): Al(1)-O(1) 1.782(1), Al(1)-N(1) 1.881(1), Al(1)-N(2) 1.888(1), Al(1)-C(32) 1.961(1), O(1)-C(34) 1.296(2), O(2)-C(34) 1.193(2), N(1)-Al(1)-N(2) 102.0(1).

While the reactivity of the Nacnac-ligated aluminium *mono*hydrides towards CO_2 is selective, the chemistry of [^{Dipp}**1**]AlH_2 with CO_2 reveals that the presence of a second aluminium-bound hydride leads to more complex chemistry. In the presence of excess CO_2, [^{Dipp}**1**]AlH_2 is rapidly consumed: after 20 min, *ca.* 40% of the compound has reacted, and the major product is thought to be [^{Dipp}**1**]Al(H){OC(O)H}, signalled by a sharp singlet, integrating to 1H, at δ_H = 8.11 ppm. This reactivity is not selective, however, and three further singlets are present in the region δ_H = 4.78 – 5.13 ppm, indicative of the formation of additional Nacnac-ligated species. [^{Dipp}**1**]AlH_2 is completely consumed over the course of several hours, leading to a mixture of species which could not be separated, including a second formate complex, giving rise to a resonance at δ_H = 8.21 ppm - possibly due to insertion of CO_2 into the second Al-H bond.

In the presence of a stoichiometric deficiency of CO_2, the same major formate signal at δ_H = 8.11 ppm is observed, although again the reaction is not selective. In this case, crystals suitable for X-ray diffraction could be obtained from the reaction mixture after several days, and shown to contain the dimeric dialuminium-acetal complex, {[^{Dipp}**1**]Al(OCH_2O)}$_2$ (see ESI), a binuclear aluminium complex with a $(AlOCH_2O)_2$ core structure, which has previously been reported by Driess *et al.* to be formed in the reaction of a germanium formate complex with [^{Dipp}**1**]AlH_2.[21] In our case, we postulate that {[^{Dipp}**1**]Al(OCH_2O)}$_2$ is formed from [^{Dipp}**1**]Al(H){OC(O)H} via intermolecular (bimolecular) hydro-alumination of the formate function. Similar chemistry is observed with reactive B-H bonds (see below) and the deficit of CO_2 presumably promotes this reaction pathway over CO_2 insertion into the second Al-H bond.

The relative reactivity of 'electronically modified' N-nacnac aluminium hydrides towards CO_2 was also probed. In contrast to its regular Nacnac counterpart, [^{Dipp}**2**]Al(H)Et reacts instantly under 1 bar of CO_2 leading to quantitative formation of [^{Dipp}**2**]Al(Et){OC(O)H}. The product is characterized by a sharp ^{1}H NMR resonance at δ_H = 8.76 ppm and a strong IR absorption at 1678 cm^{-1} characteristic of the formate group, and its structure in the solid state confirmed by X-ray crystallography (Figure 5). The reaction(s) of [^{Dipp}**2**]AlH_2 with CO_2 are also markedly faster than those of [**Dipp1**]AlH_2. Monitoring of the course of the reaction by ^{1}H NMR spectroscopy shows instant consumption of [^{Dipp}**2**]AlH_2 and selective formation of [^{Dipp}**2**]Al(H){OC(O)H}. Although not crystallographically characterized, this compound is characterized by a sharp downfield singlet at δ_H = 8.30 ppm, integrating to one hydrogen, and a shift in the broad Al-H resonance from δ_H = 4.52 ppm to δ_H = 5.22 ppm. Moreover, the signals due to the ligand backbone feature four doublets and two septets corresponding to the Dipp isopropyl groups of a N-Nacnac species that lacks C_2 symmetry, and therefore features an unsymmetrically-substituted aluminium centre. While

[^{Dipp}**2**]Al(H){OC(O)H} does not appear to dimerize to give an acetal derivative in the manner of [^{Dipp}**2**]Al(H){OC(O)H}, it does react readily with further CO_2 over 12 h to give the bis(formate) complex [^{Dipp}**2**]Al{OC(O)H}$_2$ as the only aluminium containing product.

It is apparent that the N-nacnac ligated species [^{Dipp}**2**]Al(Et)H and [^{Dipp}**2**]AlH_2 react significantly faster than their ^{Dipp}**1** counterparts with CO_2. IR data for the two series of compounds imply that the electronic differences between the two compounds are rather small. Notably the Al-H stretches for the N-nacnac compounds are very similar to (or even at slightly *higher* wavenumber than) their Nacnac analogues. This in turn would imply comparable or (if anything) slower reactivity towards CO_2. We hypothesize that the differences between the two sets of compounds are largely steric in origin, with more open access to the reactive Al-H bond being possible in the N-nacnac compounds. This in turn reflects the steric effects of the backbone NMe_2 groups. As noted previously for related group 14 complexes,[39] these amino groups exert a pronounced steric repulsion on the N-bound Dipp substitutents, causing them to be bent down significantly out of the C_3N_2 plane. Since the hydride ligand occupies the axial position in both [^{Dipp}**1**]Al(Et)H and [^{Dipp}**2**]Al(Et)H, and is projected out of the C_3N_2 plane in the opposite sense, this renders the Al-H bond less sterically protected in the N-nacnac system. As evidence for the difference in steric profiles, we note that the centroid-Al-centroid angle relating to the two flanking Dipp rings is somewhat more acute in [^{Dipp}**2**]Al(Et)H than [^{Dipp}**1**]Al(Et)H (140.0 vs. 146.7°). Moreover, the extent to which the aluminium centre is projected out of the β-diketiminate C_3N_4 plane is known to be related to steric pressures at aluminium, and it is of note therefore that in [^{Dipp}**2**]Al(Et)H, the metal lies significantly closer to the respective plane (0.464 vs 0.663 Å; Figure 6).

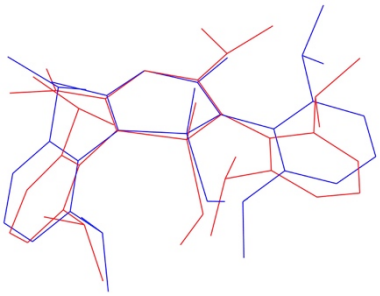

Figure 6. Overlay of the molecular structures of [^{Dipp}**1**]Al(Et)H (blue) and [^{Dipp}**2**]Al(Et)H (red) as determined by X-ray crystallography.

Reactions of aluminium formate complexes with B-H containing reductants

[^{Dipp}**1**]Ga(^{t}Bu)H operates as a catalyst for carbon dioxide reduction via insertion of CO_2 into the Ga-H bond, followed by metathesis between the Ga-O bond of the resulting formate complex and the B-H bond of pinacolborane (HBpin).[23] This latter step could be shown in independent stoichiometric studies to regenerate the active hydride species [^{Dipp}**1**]Ga(^{t}Bu)H and yield the formyl ester product, HC(O)OBpin. With this in mind, we decided to probe the reactions of our newly synthesized aluminium formate complexes with boranes, with the aim of establishing whether this could lead to Al-H bond formation, and thereby demonstrate the viability of aluminium hydride catalysts for the reduction of CO_2 by boranes. Our studies employed a range of boranes spanning a range of reactivity profiles (HBpin, HBcat, {H(9-BBN)}$_2$ and $BH_3{\cdot}SMe_2$), and focussed in the first instance on [^{Dipp}**1**]Al(Et){OC(O)H} as the formate substrate.

Pinacolborane, HBpin, proved to be resolutely unreactive towards [^{Dipp}**1**]Al(Et){OC(O)H} under any reaction conditions employed, and the addition of CO_2 to a mixture of [^{Dipp}**1**]Al(Et)H and HBpin, invariably led no further than the formation of the formate complex, with no apparent consumption of the borane. Catecholborane (HBcat) also has a track record as a reductant in the metal-hydride-catalysed reduction of CO_2 and frequently shows enhanced reactivity compared to the weaker Lewis acid HBpin.[22,47] With this in mind, its reactivity towards [^{Dipp}**1**]Al(Et){OC(O)H} was also investigated. In this case, addition of excess HBcat yields a single Nacnac-ligated species over the course of 6 h at room temperature. The ^{1}H NMR spectrum of this product is consistent with an aluminium centre bearing inequivalent substituents (one of which is the ethyl group retained from the parent formate complex) and the ^{11}B NMR spectrum shows a broad resonance at δ_B 21.5 ppm, indicative of a tri-coordinate boron centre bonded to three oxygen atoms.[48] These features are consistent with the results of X-ray crystallography (Figure 7), which reveal the product to be [^{Dipp}**1**]Al(Et)(OBcat), a Nacnac-ligated aluminium boryloxy complex. The reactivity of [^{Dipp}**1**]Al(Me){OC(O)H} towards HBcat is similar: *in situ* ^{1}H NMR spectroscopy is consistent with the formation of a single species which, based on its spectroscopic similarities to [^{Dipp}**1**]Al(Et)(OBcat), is postulated to be [^{Dipp}**1**]Al(Me)(OBcat).

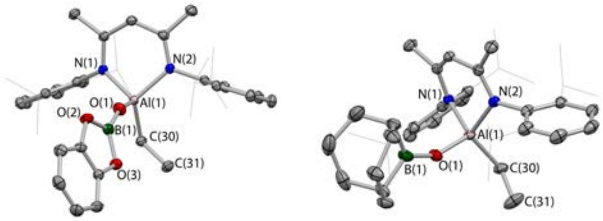

Figure 7. Molecular structures of [^{Dipp}**1**]Al(Et)(OBcat) (left) and [^{Dipp}**1**]Al(Et){O(9-BBN)} (right) as determined by X-ray crystallography. Thermal ellipsoids set at the 40% probability level. Selected hydrogen atoms, solvate molecule for [^{Dipp}**1**]Al(Et)(OBcat) and second disorder component for [^{Dipp}**1**]Al(Et){O(9-BBN)} omitted, and Dipp groups shown in wireframe for clarity. Key bond lengths (Å) and angles (°): (for [^{Dipp}**1**]Al(Et)(OBcat)): Al(1)-O(1) 1.739(1), Al(1)-N(1) 1.886(11), Al(1)-N(2) 1.901(1), Al(1)-C(30) 1.953(1), O(1)-B(1) 1.308(2), O(2)-B(1) 1.409(2), O(3)-B(1) 1.405(2), N(1)-Al(1)-N(2) 97.0(1); (for [^{Dipp}**1**]Al(Et){O(9-BBN)}): Al(1)-O(1) 1.731(1), Al(1)-N(20) 1.902(1), Al(1)-N(2) 1.908(1), Al(1)-C(30) 1.951(1), O(1)-B(1) 1.328(2), N(1)-Al(1)-N(2) 96.5(1).

Metallo-borate esters of this type have been implicated as intermediates in the borane-mediated catalytic reduction of CO_2.

There are very few structurally authenticated examples of such compounds that feature main group elements, although examples of group 14 metal(II) borate esters {(^{i}Pr$_3$Si)(Ar*)N}M-(OBpin) (M = Ge, Sn; Ar* = C$_6$H$_2$^{i}Pr-4-{C(H)Ph$_2$}$_2$-2,6) were recently reported to be formed via the addition of one equivalent of HBpin to the corresponding formate complexes.[22] In that case, it has been suggested – based on computational studies – that the metal formate reacts with HBpin to yield a germa-bora-acetal intermediate, {(^{i}Pr$_3$Si)(Ar*)N}Ge(OCH$_2$OBpin), that can react onwards *via* two potential pathways which have very similar activation energies. In one route, Ge-O/H-B σ-bond metathesis with HBpin regenerates a Ge(II) hydride and (pinBO)$_2$CH$_2$. These two species then recombine, to give {(^{i}Pr$_3$Si)(Ar*)N}Ge-(OBpin) along with MeOBpin. The proposed alternative route involves the direct extrusion of formaldehyde from {(^{i}Pr$_3$Si)(Ar*)N}Ge(OCH$_2$OBpin) via a cyclic GeOCO four-membered transition state.[14,22] Similar routes have been proposed and computationally assessed using HBcat as the reductant.[15]

With this in mind, we wanted to probe possible pathways for the formation of [**Dipp1**]Al(Et)(OBcat) from [**Dipp1**]Al(Et){OC(O)H} (Scheme 6). In the first instance the reaction with one equivalent of HBcat was examined. The reaction proceeds to completion after 48 h at room temperature, generating exclusively [**Dipp1**]Al(Et)(OBcat); no intermediates could be detected. We hypothesize that the completion of the reaction under these conditions is suggestive of the formation of [**Dipp1**]Al(Et)(OBcat) *via* the intermediate aluma-bora-acetal [Dipp**1**]Al(Et)(OCH$_2$OBcat), which then eliminates formaldehyde to give the product (pathway A). Although we could not detect the formaldehyde so generated, this pathway would be consistent (i) with the completion of the reaction in the presence of only a single equivalent of HBcat; (ii) with the formation (and spectroscopic characterization) of an intermediate analogous to [Dipp**1**]Al(Et)(OCH$_2$OBcat) in the corresponding reaction utilising {H(9-BBN)}$_2$ as the borane reductant (see below); and (iii) with

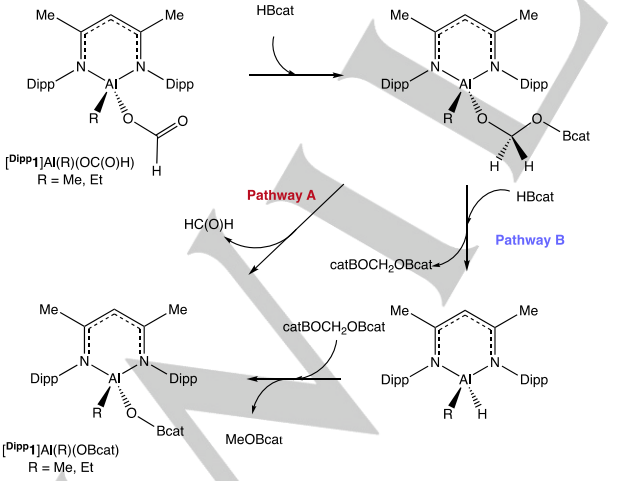

Scheme 6. Possible pathways for the formation of [Dipp**1**]Al(R)(OBcat) (R = Me, Et) from the addition of HBcat to [Dipp**1**]Al(R){OC(O)H}.

the similar extrusion of formaldehyde from the germanium complex {(^{i}Pr$_3$Si)(Ar*)N}Ge(OCH$_2$OBpin).[22] It is also worth noting that explicit experimental evidence for the production of formaldehyde has been obtained in ruthenium-catalysed CO_2 reduction chemistry.[14]

The alternative route outlined in Scheme 6 (pathway B) is not favoured in this case, on the basis of (i) the implied consumption of two equivalents of HBcat; (ii) the non-observation of the MeOBcat co-product, and (iii) the fact that it involves an Al-O/B-H metathesis step which we believe is not thermodynamically feasible using HBcat. Thus, independent assessment of the lability of systems of the type [Dipp**1**]Al(Et)(OX) (X = Me, Bcat) in the presence of excess HBcat (10 equiv.) shows no conversion to [Dipp**1**]Al(Et)H and XOBcat even after 48 h at 80°C in benzene-d$_6$. Such observations are also consistent with the lack of catalytic turnover for HBcat/CO_2 in the presence of 10 mol% [Dipp**1**]Al(Et)H, since regeneration of the Al-H bond under such conditions is not possible.

9-Borabicyclo[3.3.1]nonane {H(9-BBN)}$_2$ is another commonly employed reductant in the metal-hydride-catalysed reduction of CO_2.[46] Accordingly, the reaction of 0.5 equivalents of {H(9-BBN)}$_2$ with [Dipp**1**]Al(Et){OC(O)H} was examined; the reaction in benzene-d$_6$ reaches >95% completion after 6 h at room temperature, and selectively yields a novel species which as been characterised by NMR spectroscopy as the aluma-bora-acetal [Dipp**1**]Al(Et){OCH$_2$O(9-BBN)} (Scheme 7). Its ^{11}B NMR spectrum features a single broad resonance at δ_B = 56.0 ppm, the chemical shift of which is consistent with a 3-coordinate boron environment of the type R$_2$BOR' (cf. MeO(9-BBN): δ_B = 52.0 ppm, O(9-BBN)$_2$: δ_B = 58.2 ppm).[49,50] In addition, the ^{1}H NMR spectrum features a singlet at δ_H 5.63, integrating to two hydrogens (and correlating to a secondary carbon resonance at δ_C 87.6 ppm) assigned to the acetal functionality of the {OCH$_2$O(9-BBN)} substituent; its chemical shift is consistent with those reported for related compounds (e.g. CH$_2${O(9-BBN)}$_2$: δ_H = 5.34 ppm, CH$_2$(OBpin)$_2$ δ_H = 5.49 ppm).[12,51] The corresponding systems [Dipp**1**]Al(Me){OCH$_2$O(9-BBN)} and [Dipp**2**]Al(Et){OCH$_2$O(9-BBN)} can be synthesised using analogous methods and characterised by NMR spectroscopy. The diagnostic ^{1}H, ^{11}B and ^{13}C resonances associated with the {OCH$_2$O(9-BBN)} function appear at essentially identical chemical shifts for all three compounds.

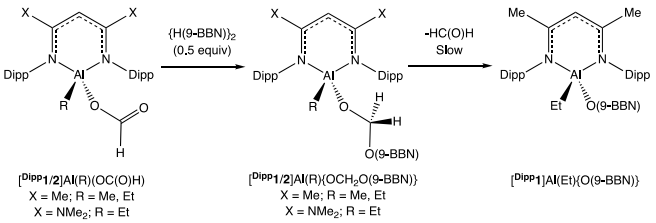

Scheme 7. Formation and onward reactivity of aluma-bora-acetals through the formal hydroboration of formate C=O bonds using {H(9-BBN)}$_2$.

Complexes of this nature have frequently been postulated as intermediates in the borane-mediated catalytic reduction of CO_2,[22] and the formation of [^{Dipp}**1**]Al(Et)(OBcat) is hypothesised to proceed *via* the closely related intermediate [^{Dipp}**1**]Al(Et){OCH_2O(Bcat)}. However, acetals of this type are rarely observed experimentally; typically, such species are not persistent in solution due to their propensity to undergo further σ-bond metathesis reactions across the M-O bond or to eliminate formaldehyde to yield a metal borate ester. In the case of [^{Dipp}**1**]Al(Et){OCH_2O(9-BBN)}, the difference in stability compared to its putative Bcat analogue [^{Dipp}**1**]Al(Et){OCH_2O(Bcat)} is striking. While the latter cannot even be detected as an intermediate on the pathway to [**^{Dipp}1**]Al(Et)(OBcat), its 9-BBN counterpart undergoes the analogous loss of formaldehyde very slowly indeed. [^{Dipp}**1**]Al(Et){OCH_2O(Bcat)} is stable in solution at room temperature for up to 32 h but over longer periods (*ca.* 2 weeks) a significant level of degradation is observed resulting in the formation of [^{Dipp}**1**]Al(Et){O(9-BBN)} (Scheme 7). The elimination of HC(O)H from species of the type [^{Dipp}**1**]Al(Et){$OCH_2O(BX_2)$} necessarily involves the cleavage of either the Al-O or B-O bond. The very different stabilities of the 9-BBN and Bcat systems of this type implies that the boron-bound substituents play a significant role in modulating lability, and we therefore favour a mechanism involving B-O bond cleavage (Scheme 8). The much longer-lived nature of the 9-BBN derivative would then be in line with the stronger B-O bond expected in association with a *dialkyl* BX_2 function.

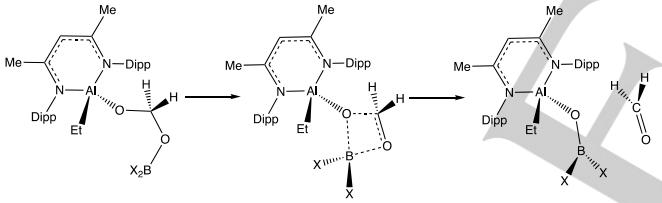

Scheme 8. Proposed mechanism for the conversion of an aluma-bora-acetal to the corresponding boryloxy species via B-O bond cleavage (BX_2 = Bcat, 9-BBN)

The product of formaldehyde loss, [^{Dipp}**1**]Al(Et){O(9-BBN)}, has been characterized by standard analytical and spectroscopic techniques and its structure in the solid state determined by X-ray crystallography (Figure 7). Geometrically, the molecular structure closely resembles that of [^{Dipp}**1**]Al(Et)(OBcat) with only minor differences in the geometry at the aluminium centre.

In view of the formation of [^{Dipp}**1**]Al(Et){OCH_2O(9-BBN)} from the reaction of [**^{Dipp}1**]Al(Et){OC(O)H} with stoichiometric {H(9-BBN)}$_2$, we were keen to examine whether the acetal species would undergo further reaction with excess borane under more forcing conditions. In particular – given the more reactive nature of {H(9-BBN)}$_2$ compared to HBcat, we were interested to see if any evidence could be found for metathetical regeneration of an Al-H bond. At room temperature, however, [^{Dipp}**1**]Al(Et){OCH_2O(9-BBN)} exhibits minimal onward reactivity over several days even in the presence of excess {H(9-BBN)}$_2$. By contrast, complete consumption of the acetal occurs when the reaction mixture is heated to 80°C for 4 d. The ^{1}H NMR spectrum of the product mixture is consistent with the presence of two major Nacnac-ligated species. One of these can be identified as identified as [^{Dipp}**1**]Al(Et){O(9-BBN)}, the formation of which is accompanied by the generation of the known compound MeO(9-BBN).[13,49] The other major Nacnac-containing species gives rise to a singlet at δ_H 3.85 ppm which integrates to three protons, the chemical shift being consistent with a methoxide resonance. The identity of this species was subsequently confirmed as [^{Dipp}**1**]Al(Et)(OMe) through independent synthesis from [**^{Dipp}1**]Al(Et)H and methanol (see ESI). It is important to note that we see no evidence for the formation of any Al-H containing species, nor for the presence of CH_2{O(9-BBN)}$_2$, suggesting that σ-bond metathesis does not occur across the Al-O bond.

Instead, we propose that the observed product profile arises from B-H/C-O σ-bond metathesis across either C-O bond of the {OCH_2O(9-BBN)} functionality of [^{Dipp}**1**]Al(Et){OCH_2O(9-BBN)}, yielding either [^{Dipp}**1**]Al(Et){O(9-BBN)} and MeO(9-BBN), or [^{Dipp}**1**]Al(Et)(OMe) and O(9-BBN)$_2$ (Scheme 9). These pathways are apparently feasible in the absence of accessible Al-O/B-H metathetical pathways, but presumably incur relatively high activation barriers, consistent with the high temperature and long reaction times required to bring about consumption of [**^{Dipp}1**]Al(Et){OCH_2O(9-BBN)}.

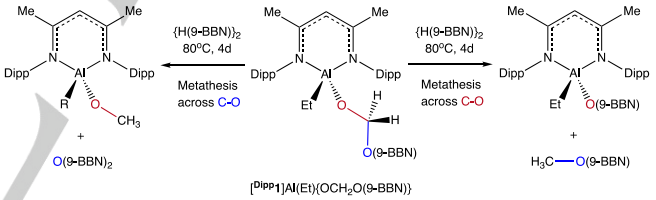

Scheme 9. Proposed routes for formation of the observed Nacnac-containing products in the reaction of [^{Dipp}**1**]Al(Et){OCH_2O(9-BBN)} with excess {H(9-BBN)}$_2$ at 80°C.

While BH_3-containing reagents are commonly used in the hydroboration of unsaturated carbon-element bonds, they have been much less widely employed in the catalytic reduction of CO_2.[52] The first reported deployment of $BH_3{\cdot}SMe_2$ was in the reduction of CO_2 catalysed by the borane/phosphine FLP, 1-Bcat-2-PPh_2-C_6H_4.[53,54] The successful use $BH_3{\cdot}SMe_2$ in conjunction with metal hydrides for the reduction of CO_2 has to our knowledge, not been reported, despite potential merits relating to its inexpensive nature and enhanced reactivity. As such we probed its reactivity towards aluminium formates. The reaction of [**^{Dipp}1**]Al(Et){OC(O)H} with excess $BH_3{\cdot}SMe_2$ (3 equiv.) at room temperature proceeds to > 95% conversion after 3 h. The resulting ^{1}H NMR spectrum is indicative of the presence of one major and two minor Nacnac-ligated species (in approximate ratio 5:1:1). The major product could be crystallised from *n*-hexane and its identity elucidated by X-ray crystallography, revealing that it is [**^{Dipp}1**]Al(Et){OB(H)OMe} (Scheme 10 and Figure 8).

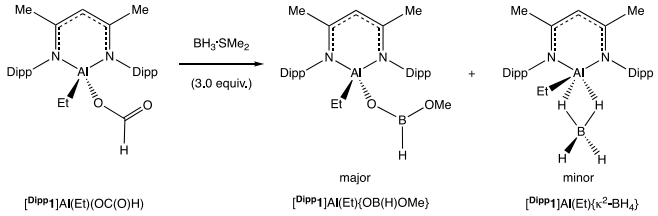

Scheme 10. Reaction of [**Dipp1**]Al(Et){OC(O)H} with excess $BH_3{\cdot}SMe_2$.

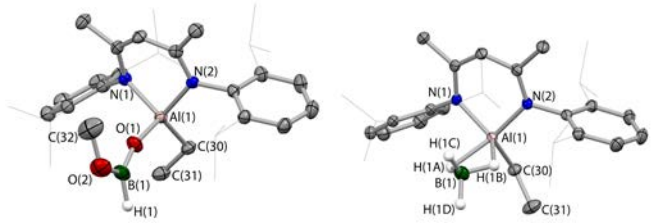

Figure 8. Molecular structures of [Dipp**1**]Al(Et){OB(H)OMe} (left) and [Dipp**1**]Al(Et)(κ^2-BH_4) (right) as determined by X-ray crystallography. Thermal ellipsoids set at the 40% probability level. Selected hydrogen atoms omitted and Dipp groups shown in wireframe for clarity. B-H and Al-H-B hydrogens located in the difference Fourier map and refined isotropically. Key bond lengths (Å) and angles (°): (for [Dipp**1**]Al(Et){OBH(OMe)}): Al(1)-O(1) 1.725(2), Al(1)-N(1) 1.904(2), Al(1)-N(2) 1.896(1), Al(1)-C(30) 1.960(2), O(1)-B(1) 1.318(2), O(2)-B(1) 1.357(3), N(2)-Al(1)-N(1) 96.9(1); (for [Dipp**1**]Al(Et)(κ^2-BH_4)): Al(1)-B(1) 2.234(2), Al(1)-N(1) 1.916(1), Al(1)-N(2) 1.910(1), Al(1)-C(30) 1.971(2), Al(1)-H(1A) 1.84(2), Al(1)-H(1B) 1.78(2), B(1)-H(1A) 1.16(2), B(1)-H(1B) 1.18(3), B(1)-H(1C) 1.04(3), B(1)-H(1D) 1.12(2).

The molecular structure of [**Dipp1**]Al(Et){OB(H)OMe} features a tetra-coordinate aluminium centre, ligated by Nacnac and ethyl donors, and an unusual borate ligand, {OB(OMe)H}, featuring a trigonal boron centre and pendant H/OMe substituents. The B-H hydrogen was located in the difference Fourier map and refined isotropically; the B-H distance is consistent with those reported in the literature.[55] Spectroscopically, the OMe substituent is characterized by a ^{1}H NMR singlet at δ_H = 3.63 ppm, integrating to three protons and correlating to a primary carbon resonance at δ_C = 50.0 ppm. A broad ^{1}H resonance is observed in the ^{1}H{^{11}B} NMR spectrum at δ_H = 4.77 ppm and the ^{11}B NMR spectrum shows a broad signal at δ_B = 25.1 ppm which narrows markedly upon ^{1}H decoupling (from $\Delta\omega_{1/2}$ 1102 Hz to $\Delta\omega_{1/2}$ 458 Hz.). In addition, the IR spectrum features a B-H stretch at 2434 cm^{-1} consistent with the presence of a terminal B-H bond.[56]

The mechanism for the formation of [**Dipp1**]Al(Et){OB(H)OMe} from [**Dipp1**]Al(Et){OC(O)H} and $BH_3{\cdot}SMe_2$ is clearly of some interest. Based on the observed reactivity towards HBcat and {H(9-BBN)}$_2$, we postulate that this proceeds initially via the formation of an acetal derivative which extrudes formaldehyde to give the corresponding borate species featuring the Al-O-B linkage observed in the final product (Scheme 11). In contrast to the analogous product, [**Dipp1**]Al(Et)(OBcat), obtained in the reaction with HBcat, this putative species would contain reactive B-H bonds, and the recapture of HC(O)H via a net hydroboration process would then generate the observed BOMe unit.

Interestingly, one of the minor products from the reaction of [**Dipp1**]Al(Et){OC(O)H} with excess $BH_3{\cdot}SMe_2$ (formed in ca. 14% yield) gives rise to a high field quintet in the ^{11}B spectrum (δ_B −37 ppm, $^1J_{BH}$ = 84 Hz) and can be shown by comparison with an authentic sample to be the borohydride complex [**Dipp1**]Al(Et)(κ^2-BH_4). This compound can be synthesized independently via the reaction of [**Dipp1**]Al(Et)H with $BH_3{\cdot}SMe_2$ and has been crystallographically characterized (Figure 8). Moreover, its identification in the product mixture derived from the reaction of the same borane with [**Dipp1**]Al(Et){OC(O)H} implies that – albeit to a minor extent – Al-O/B-H metathesis is

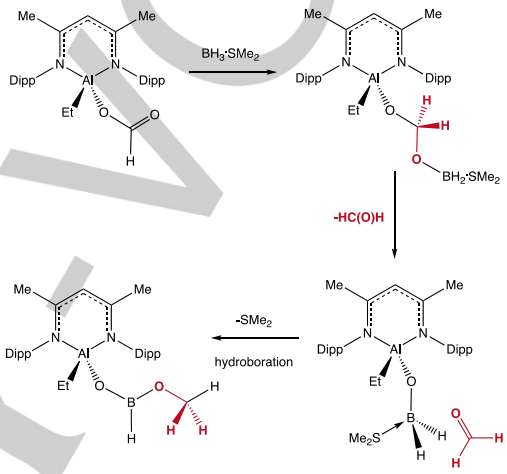

Scheme 11. Proposed routes for the formation of [**Dipp1**]Al(Et){OB(H)OMe} in the reaction of [**Dipp1**]Al(Et){OC(O)H} with excess $BH_3{\cdot}SMe_2$.

viable in this system. Given that no other examples of such a process could be identified with the other boranes examined in this study, and that the BH_3 fragment is very strongly Lewis acidic, it is conceivable that an additional thermodynamic driver involves the interaction of the Al-H bond with the BH_3 fragment to give a borohydride product. In the absence of such an interaction, tabulated E-H/E-O bond strengths for E = B, Al (E-H: 377, 282 kJ mol^{-1}; E-O: 559, 585 kJ mol^{-1}) suggest that Al-O/B-H metathesis is highly thermodynamically unfavourable.[57]

In terms of the pathway(s) for the formation of the borohydride complex, reactions of [**Dipp1**]Al(Et){OB(H)OMe} with excess $BH_3{\cdot}SMe_2$ – even under forcing conditions – do not lead to conversion to [**Dipp1**]Al(Et)(κ^2-BH_4). The borohydride system appears to be formed via a process parallel to that leading to the formation of the major product. As such, release of the {OB(H)OMe} unit via Al-H bond formation does not appear feasible, and the possibility for catalytic conversion in the $BH_3{\cdot}SMe_2/CO_2$ system using [**Dipp1**]Al(Et)H is ruled out.

Conclusions

A range of novel β-diketiminate stabilized aluminium hydrides of the type (Nacnac)Al(R)H has been synthesized offering variation

in the auxiliary R substituent and in the Nacnac backbone itself. These show significant variation in the nature of the Al-H bond – as revealed by a wide spread in their measured IR stretching frequencies – and consequently marked differences in reactivity with respect to the insertion of CO_2. Electron-donating R groups give rise to weaker (and presumably more hydridic) Al-H bonds, leading to enhanced rates of reactivity towards CO_2.

With a view to probing the viability of the steps needed for catalytic turnover in the reduction of CO_2, the reactions of [**Dipp1**]Al(Et){OC(O)H} with a range of boranes have been investigated. In the case of pinacolborane, no reactivity is observed even under forcing conditions. HBcat and $\{H(9\text{-BBN})\}_2$ ultimately give products of the type [**Dipp1**]Al(Et)(OBX_2) involving cleavage of one of the C-O bonds in CO_2. In the $\{H(9\text{-BBN})\}_2$ case, this chemistry can be shown explicitly to proceed via an acetal intermediate of the type [**Dipp1**]Al(Et){OCH_2O(9-BBN)}. Under forcing conditions in the presence of excess $\{H(9\text{-BBN})\}_2$, this species is cleaved to give products ([**Dipp1**]Al(Et){O(9-BBN)} and [**Dipp1**]Al(Et)(OMe) - in which the Al-O bond is invariably retained. In the case of $BH_3{\cdot}SMe_2$, the major product, [**Dipp1**]Al(Et){OB(H)OMe}, also features an Al-O-B unit; this system does, however, provide the only experimental evidence for the regeneration of an Al-H bond. Thus, a minor product can be shown to be the borohydride complex [**Dipp1**]Al(Et)(κ^2-BH_4). We propose that the additional interaction of the strongly Lewis acidic BH_3 unit with the aluminium hydride (to give a borohydride ligand) is a key thermodynamic driver in generating this product from [**Dipp1**]Al(Et){OC(O)H}. In the absence of such an interaction, literature tabulated E-H/E-O bond strengths for E = B, Al suggest that Al-O/B-H metathesis is likely to be thermodynamically unfavourable (> +120 kJ mol^{-1}), in agreement with our experimental observations with HBpin, HBcat and $\{H(9\text{-BBN})\}_2$.[56] As a point of reference, the corresponding data for gallium (Ga-H: 260 kJ mol^{-1}; Ga-O: 430 kJ mol^{-1})[57] imply that Ga-O/B-H metathesis should be thermodynamically favourable (albeit marginally so). This hypothesis is in line with the experimental observations (i) that catalytic turnover is possible in the [**Dipp1**]Ga(^{t}Bu)H/CO_2/borane system; and (ii) that (unlike its aluminium counterparts) [**Dipp1**]Ga(Ph)(OMe) reacts with the least activated borane, HBpin, to generate [**Dipp1**]Ga(Ph)H in a timeframe of < 5 min.

Experimental Section

General details

All manipulations were carried out using standard Schlenk line or dry-box techniques under an atmosphere of argon. Solvents were degassed by sparging with argon and dried by passing through a column of the appropriate drying agent using a commercially available Braun SPS. NMR spectra were measured in benzene-d_6 which was dried over potassium and stored under argon in a Teflon valve ampoule. NMR samples were prepared under argon in 5 mm Wilmad 507-PP tubes fitted with J. Young Teflon valves. NMR spectra were measured on Varian Mercury-VX-300 or Bruker AVII-500 spectrometers; ^{1}H and ^{13}C NMR spectra were referenced internally to residual protio-solvent (^{1}H) or solvent (^{13}C) resonances and are reported relative to tetramethylsilane (δ□= 0 ppm). ^{11}B and ^{27}Al NMR spectra were referenced with respect to $BF_3{\cdot}OEt_2$ and $[Al(H_2O)_6]^{3+}$, respectively. Chemical shifts are quoted in δ (ppm) and coupling constants in Hz. Elemental analyses were carried out at London Metropolitan University. The syntheses of [**Dipp1**]Al(Et)Cl, [**Dipp1**]$AlCl_2$, [**Dipp1**]AlH_2, [**Dipp2**]H and $Me_3N{\cdot}AlH_3$ were carried out as per literature precedent.[39,40-42,58,59]

Crystallographic details

JH[60]

Syntheses of novel compounds

(Key compounds are included here; see ESI for further synthetic/characterizing data)

[Dipp1]Al(Et)H: [**Dipp1**]Al(Et)Cl (3.250 g, 6.38 mmol) was dissolved in diethyl ether and cooled to −78ºC. A solution of $LiAlH_4$ (0.242 g, 6.38 mmol), also in diethyl ether, was added dropwise and, upon complete addition, the reaction mixture was allowed to warm to room temperature. The yellow solution decolourised and evolved a white precipitate. After further stirring at room temperature for 5 h, the reaction mixture was filtered and volatiles removed *in vacuo* to yield a white residue. The residue was extracted into *n*-hexane, filtered (leaving a colourless precipitate that reacted violently with water), and the filtrate concentrated until the point of incipient crystallisation. Storage of the hexane solution at 6ºC for several hours yields large, colourless, single crystals, suitable for X-ray crystallography. The isolation of the crystals, and further concentration and cooling of the supernatant yielded a second crop of large crystals. Yield: 2.40 g, 79%. ^{1}H NMR (400 MHz, benzene-d_6, 298 K): δ_H −0.13 (2H, q, $^3J_{HH}$ = 8.2 Hz, $CH_3C\underline{H}_2Al$), 0.79 (3H, t, $^3J_{HH}$ = 8.2 Hz, $C\underline{H}_3CH_2Al$), 1.11 (6H, d, $^3J_{HH}$ = 6.8 Hz, CH_3 of Dipp ^{i}Pr), 1.17 (6H, d, $^3J_{HH}$ = 6.8 Hz, CH_3 of Dipp ^{i}Pr), 1.35 (6H, d, $^3J_{HH}$ = 6.8 Hz, CH_3 of Dipp ^{i}Pr), 1.39 (6H, d, $^3J_{HH}$ = 6.8 Hz, CH_3 of Dipp ^{i}Pr), 1.56 (6H, s, CH_3 of β-diketiminato backbone), 3.34 (2H, sept, $^3J_{HH}$ = 6.8 Hz, CH of Dipp ^{i}Pr), 3.51 (2H, sept, $^3J_{HH}$ = 6.8 Hz, CH of Dipp ^{i}Pr), 4.57 (1H, br s, AlH), 4.92 (1H, s, γ-CH), 7.08-7.15 (6H, m, aromatic CH). ^{13}C{^{1}H} NMR (101 MHz, benzene-d_6, 298 K): δ_C –0.9 (br, $CH_3\underline{C}H_2Al$), 9.1 ($\underline{C}H_3CH_2Al$) 23.0 (CH_3 of β-diketiminato backbone), 24.2, 24.4, 24.9, 26.4 (CH_3 of Dipp ^{i}Pr), 28.2, 28.9 (CH of Dipp ^{i}Pr), 97.0 (γ-CH), 124.1, 124.9, 127.3, 140.5, 143.6, 145.2 (ArC of Dipp), 170.0 (NC). ^{27}Al NMR (104 MHz, benzene-d_6, 298 K): δ_{Al} not observed. EI-MS: *m/z* calc for $C_{29}H_{42}N_2Al$ ([M-Et]$^+$) 445.3163, meas. 445.3155 (100%), calc. for $C_{31}H_{46}N_2Al$ ([M-H]$^+$) (20%). IR (nujol/cm^{-1}) $\nu_{Al\text{-}H}$: 1776 (s). Elemental microanalysis: calc. for $C_{31}H_{47}N_2Al$: C 78.44% H 9.98% N 5.90% meas. C 78.10% H 9.89% N 5.75%. Crystallographic data: $C_{31}H_{47}N_2Al$ (M_r = 474.68): monoclinic, *P* $2_1/c$, *a* = 10.64370(10), *b* = 12.5456(2), *c* = 22.5672(3) Å, β = 98.6340(10) °, *V* = 2979.28(7) Å^3, *Z* = 4, ρ_c = 1.058 g cm^{-3}, *T* = 150(2) K, λ = 1.54184 Å, μ(Cu Kα) = 0.723 mm^{-1}, 16633 reflections collected, 6164 independent [R(int) = 0.0408] used in all calculations. R_1 = 0.0526, wR_2 = 0.1397 for observed unique reflections [$I > 2\sigma(I)$] and R_1 = 0.0618, wR_2 = 0.1514 for all

unique reflections. Max. and min. residual electron densities 0.497, −0.278 e Å^{-3}.

[^{Dipp}1]Al(Cl)H: To a solution of [^{Dipp}**1**]AlCl$_2$ (3.00 g, 5.82 mmol) in diethyl ether (40 mL) at −78°C was added dropwise a solution of LiAlH$_4$ (0.221 g, 5.82 mmol), also in diethyl ether (20 mL). The reaction mixture was allowed to warm to room temperature and stirred for 90 min, over which time the yellow solution decolourised, and a colourless precipitate was formed. Volatiles were removed *in vacuo* and the white solid residue extracted with *n*-hexane. The resulting slurry was filtered (leaving behind a colourless residue that reacted violently with water), concentrated to the point of incipient crystallisation and cooled to −30°C. Storage of this solution at this temperature overnight yielded colourless block-like crystals, suitable for X-ray diffraction. Yield: 2.15 g, 77%. ^{1}H NMR (400 MHz, benzene-d$_6$, 298 K): δ$_H$ 1.10 (6H, d, $^3J_{HH}$ = 6.8 Hz, CH$_3$ of Dipp ^{i}Pr), 1.13 (6H, d, $^3J_{HH}$ = 6.8 Hz, CH$_3$ of Dipp ^{i}Pr), 1.34 (6H, d, $^3J_{HH}$ = 6.8 Hz, CH$_3$ of Dipp ^{i}Pr), 1.47 (6H, d, $^3J_{HH}$ = 6.8 Hz, CH$_3$ of Dipp ^{i}Pr), 1.52 (6H, s, CH$_3$ of β-diketiminato backbone), 3.30 (2H, sept, $^3J_{HH}$ = 6.8 Hz, CH of Dipp ^{i}Pr), 3.47 (2H, sept, $^3J_{HH}$ = 6.8 Hz, CH of Dipp ^{i}Pr), 4.55 (1H, br s, Al-H), 4.88 (1H, s, γ-CH), 7.06-7.17 (6H, m, aromatic CH). ^{13}C{^{1}H} NMR (101 MHz, benzene-d$_6$, 298 K): δ$_C$ 23.3 (CH$_3$ of β-diketiminato backbone), 24.7, 24.9, 25.3, 25.5 (CH$_3$ of Dipp ^{i}Pr), 28.6, 28.9 (CH of Dipp ^{i}Pr), 97.70 (γ-CH), 124.7, 125.1, 127.9, 138.7, 144.1, 145.3 (ArC of Dipp), 171.2 (NC). ^{27}Al NMR (104 MHz, benzene-d$_6$, 298K): δ$_{Al}$ 116. EI-MS: *m/z* calc for C$_{29}$H$_{51}$N$_2$AlCl ([M-H]$^+$) 479.2774, meas. 479.2752 (70%). IR (nujol/cm^{-1}) ν$_{Al-H}$: 1865, 1842 (s). Elemental microanalysis: calc. for C$_{29}$H$_{42}$N$_2$AlCl: C 72.40% H 8.80% N 5.82% meas. C 72.10% H 8.70% N 5.67%. Crystallographic data: C$_{29}$H$_{42}$N$_2$AlCl (M_r = 481.08): monoclinic, *P* 2$_1$/c, *a* = 17.1474(2), *b* = 13.15230(10), *c* = 13.4004(2) Å, β = 108.8020(10) °, *V* = 2860.89(6) Å^3, *Z* = 4, ρ_c = 1.115 g cm^{-3}, *T* = 150(2) K, λ = 1.54184 Å, μ(Cu Kα) = 1.599 mm^{-1}, 18134 reflections collected, 5908 independent [R(int) = 0.0185] used in all calculations. R_1 = 0.0570, wR_2 = 0.1312 for observed unique reflections [$I > 2\sigma(I)$] and R_1 = 0.0592, wR_2 = 0.1328 for all unique reflections. Max. and min. residual electron densities 1.165, −1.082 e Å^{-3}.

[^{Dipp}2]AlH$_2$: To a stirred solution of Me$_3$N·AlH$_3$ (0.130 g, 1.46 mmol) in toluene (10 mL) at 0°C was added dropwise a solution of [^{Dipp}**2**]H (0.500 g, 1.05 mmol), also in toluene (15 mL). The reaction mixture was allowed to warm to room temperature and stirred for 24 h, after which time the solution was filtered and volatiles removed *in vacuo*. The resulting white solid was extracted into hexane, filtered to remove traces of Me$_3$N·AlH$_3$, and volatiles removed *in vacuo* to yield a spectroscopically pure white powder. Colourless acicular crystals, suitable for X-ray crystallography, were obtained from the storage of a saturated solution in *n*-hexane at −30°C overnight. The crystals were isolated and dried *in vacuo*. A second crop of crystals was obtained on further concentration of the supernatant solution and storage at −30°C. Yield: 0.34 g, 64%. ^{1}H NMR (400 MHz, benzene-d$_6$, 298 K): δ$_H$ 1.19 (12H, d, $^3J_{HH}$ = 6.8 Hz, CH$_3$ of Dipp ^{i}Pr), 1.43 (12H, d, $^3J_{HH}$ = 6.8 Hz, CH$_3$ of Dipp ^{i}Pr), 2.20 (12H, s, CH$_3$ of NMe$_2$), 3.58 (4H, sept, $^3J_{HH}$ = 6.8 Hz, CH of Dipp ^{i}Pr), 3.84 (1H, s, γ-CH), 4.52 (2H, br s, AlH), 7.11 (6H, s, aromatic CH). ^{13}C{^{1}H} NMR (101 MHz, benzene-d$_6$, 298 K): δ$_C$ 23.8, 26.8 (CH$_3$ of Dipp ^{i}Pr), 28.6 (CH of Dipp ^{i}Pr), 40.9 (CH$_3$ of NMe$_2$) 75.3 (γ-CH), 124.7, 125.9, 141.8, 144.8 (ArC of Dipp), 166.9 (NC). ^{27}Al NMR (104 MHz, benzene-d$_6$, 298 K): δ$_{Al}$ not observed. EI-MS: *m/z* calc for C$_{31}$H$_{48}$N$_4$Al ([M-H]$^+$) 503.3689, meas. 503.3686 (5%). IR (nujol/cm^{-1}) ν$_{Al-H}$: 1840, 1793. Elemental microanalysis: calc. for C$_{31}$H$_{49}$N$_4$Al: C 73.77% H 9.79% N 11.10% meas. C 73.56% H 9.43% N 10.89%. Crystallographic data: C$_{31}$H$_{49}$N$_4$Al (M_r = 504.74): monoclinic, *P*2$_1$/*n*, *a* = 15.7577(3), *b* = 16.3675(3), *c* = 24.5939(5) Å, β = 100.989(2) °, *V* = 6226.8(2) Å^3, *Z* = 8, ρ_c = 1.077 g cm^{-3}, *T* = 150 K, μ(Cu Kα) = 0.736 mm^{-1} , λ = 1.54184 Å. 63382 reflections collected, 12911 independent [R(int) = 0.044] used in all calculations. R_1 = 0.0403, wR_2 = 0.1022 for observed unique reflections [$I > 2\sigma(I)$] and R_1 = 0.0576, wR_2 = 0.1129 for all unique reflections. Max. and min. residual electron densities 0.40, −0.37 e Å^{-3}.

[^{Dipp}2]Al(Et)H: To a stirred solution of [^{Dipp}**2**]Al(Et)Cl (2.80 g, 4.94 mmol) in diethyl ether (30 mL) at –78°C was added dropwise a solution of LiAlH$_4$ (0.280 g, 7.38 mmol) in diethyl ether (10 mL). The reaction mixture was allowed to attain room temperature and stirred for 24 h, over which time a colourless precipitate was formed. The resulting solution was filtered, and volatiles removed *in vacuo.* The residual solid was extracted with toluene, dried *in vacuo*, and then re-extracted into *n*-hexane. The solution was filtered, concentrated to incipient crystallisation and cooled to −30°C, yielding colourless plate-like crystals suitable for X-ray crystallography. The crystals were filtered and dried *in vacuo*. Further concentration of the supernatant solution and storage at −30°C produced a second crop of crystals. Yield: 1.36 g, 52%. ^{1}H NMR (400 MHz, benzene-d$_6$, 298 K): δ$_H$ –0.24 (2H, q, $^3J_{HH}$ = 8.2 Hz, CH$_3$C<u>H$_2$</u>Al), 0.74 (3H, t, $^3J_{HH}$ = 8.2 Hz, C<u>H$_3$</u>CH$_2$Al), 1.15 (6H, d, $^3J_{HH}$ = 6.7 Hz, CH$_3$ of Dipp ^{i}Pr), 1.23 (6H, d, $^3J_{HH}$ = 6.7 Hz, CH$_3$ of Dipp ^{i}Pr), 1.34 (6H, d, $^3J_{HH}$ = 6.7 Hz, CH$_3$ of Dipp ^{i}Pr), 1.59 (6H, d, $^3J_{HH}$ = 6.7 Hz, CH$_3$ of Dipp ^{i}Pr), 2.22 (12H, s, CH$_3$ of NMe$_2$), 3.09 (2H, sept, $^3J_{HH}$ = 6.7 Hz, CH of Dipp ^{i}Pr), 3.67 (1H, s, γ-CH), 4.05 (2H, sept, $^3J_{HH}$ = 6.7 Hz, CH of Dipp ^{i}Pr), 4.90 (1H, br s, AlH), 7.11 – 7.17 (6H, m, aromatic CH). ^{13}C{^{1}H} NMR (101 MHz, benzene-d$_6$, 298 K): δ$_C$ 1.2 (br, CH$_3$<u>C</u>H$_2$Al), 9.9 (<u>C</u>H$_3$CH$_2$Al), 24.2, 24.4, 26.5, 26.6 (CH$_3$ of Dipp ^{i}Pr), 28.3, 28.5 (CH of Dipp ^{i}Pr), 41.0 (CH$_3$ of NMe$_2$) 75.1 (γ-CH), 124.5, 125.0, 125.9, 142.1, 144.1, 145.3 (ArC of Dipp), 166.6 (NC). ^{27}Al NMR (104 MHz, benzene-d$_6$, 298 K): δ$_{Al}$ not observed. IR (nujol/cm^{-1}) ν$_{Al-H}$: 1788 (s). Elemental microanalysis: calc. for C$_{33}$H$_{53}$N$_4$Al: C 74.39% H 10.03% N 10.52% meas. C 74.24% H 9.89% N 10.42%. Crystallographic data: C$_{33}$H$_{53}$N$_4$Al (M_r = 532.77): monoclinic, *P*2$_1$/*n*, *a* = 15.3307(2), *b* = 11.9311(2), *c* = 18.5300(3) Å, β = 101.2480(10) °, *V* = 3324.26(9) Å^3, *Z* = 4, ρ_c = 1.065 g cm^{-3}, *T* = 150 K, μ(Cu Kα) = 0.712 mm^{-1}, λ = 1.54184 Å. 18678 reflections collected, 6863 independent [R(int) = 0.0263] used in all calculations. R_1 = 0.0410, wR_2 = 0.1158 for observed unique reflections [$I > 2\sigma(I)$] and R_1 = 0.0468, wR_2 = 0.1223 for all unique reflections. Max. and min. residual electron densities 0.63, −0.39 e Å^{-3}.

[^{Dipp}1]Al(Et){OC(O)H}: [^{Dipp}**1**]Al(Et)H (1.50 g, 3.16 mmol) was dissolved in toluene (10 mL) in an ampoule fitted with a J.

Young's valve and degassed by three freeze-pump-thaw cycles. The ampoule was then back-filled with carbon dioxide (*ca.* 1 bar) and stirred at room temperature for 5 h. The reaction mixture was then filtered and concentrated slightly. Storage of the solution at −30°C produced fine, colourless, acicular crystals over the course of several hours, which were isolated and dried *in vacuo*. Yield: 1.47 g, 90%. Storage of a concentrated solution in *n*-hexane at −30°C for three days yielded single, colourless, block-crystals of the hexane hemi-solvate suitable for X-ray crystallography. ^{1}H NMR (400 MHz, benzene-d_6, 298 K): δ_H −0.15 (2H, q, $^{3}J_{HH}$ = 8.1 Hz, $CH_3C\underline{H}_2Al$), 0.74 (3H, t, $^{3}J_{HH}$ = 8.1 Hz, $C\underline{H}_3CH_2Al$), 1.03 (6H, d, $^{3}J_{HH}$ = 6.8 Hz, CH_3 of Dipp ^{i}Pr), 1.19 (6H, d, $^{3}J_{HH}$ = 6.8 Hz, CH_3 of Dipp ^{i}Pr), 1.31 (12H, 2 x overlapping d, $^{3}J_{HH}$ = 6.8 Hz, 2 x CH_3 of Dipp ^{i}Pr), 1.57 (6H, s, CH_3 of β-diketiminato backbone), 3.19 (2H, sept, $^{3}J_{HH}$ = 6.8 Hz, CH of Dipp ^{i}Pr), 3.41 (2H, sept, $^{3}J_{HH}$ = 6.8 Hz, CH of Dipp ^{i}Pr), 5.25 (1H, s, γ-CH), 7.00-7.15 (6H, m, aromatic CH), 8.49 (1H, s, Al{OC(O)H}. ^{13}C{^{1}H} NMR (101 MHz, benzene-d_6, 298 K): δ_C –3.2 (br, $CH_3\underline{C}H_2Al$), 8.6 ($\underline{C}H_3CH_2Al$) 23.3 (CH_3 of β-diketiminato backbone), 24.0, 24.4, 24.9, 25.9 (CH_3 of Dipp ^{i}Pr), 27.3, 29.2 (CH of Dipp ^{i}Pr), 100.1 (γ-CH), 124.1, 125.1, 127.7, 140.0, 143.5, 145.6 (ArC of Dipp), 162.7 (Al{OC(O)H}, 171.0 (NC). ^{27}Al NMR (104 MHz, benzene-d_6, 298 K): δ_{Al} not observed. EI-MS: *m/z* calc for $C_{30}H_{42}N_2AlO_2$ ([M-Et]$^+$) 489.3062, meas. 489.3057 (80%), $C_{29}H_{42}N_2AlO$ ([M-Et-CO]$^+$) 461.3113, meas. 461.3312 (100%). IR (nujol/cm^{-1}) $\nu_{C=O}$: 1680 (s). Elemental microanalysis: calc. for $C_{32}H_{47}N_2AlO_2$: C 74.10% H 9.13% N 5.40% meas. C 73.80% H 8.92% N 5.36%. Crystallographic data: $C_{32}H_{47}N_2AlO_2{\cdot}0.5C_6H_{14}$ (M_r = 561.78): monoclinic, *P* 2$_1$/*n*, *a* = 8.61630(10), *b* = 18.55570(10), *c* = 21.66770(10) Å, β = 99.7800(10) °, *V* = 3413.92(5) Å^3, *Z* = 4, ρ_c = 1.093 g cm^{-3}, *T* = 150(2) K, λ = 1.54184 Å, μ(Cu Kα) = 0.745 mm^{-1}, 62820 reflections collected, 7099 independent [R(int) = 0.0395] used in all calculations. R_1 = 0.0373, wR_2 = 0.1011 for observed unique reflections [$I > 2\sigma(I)$] and R_1 = 0.0393, wR_2 = 0.1032 for all unique reflections. Max. and min. residual electron densities 0.315, −0.262 e Å^{-3}.

Reaction of [^{Dipp}1]AlH$_2$ with CO$_2$: isolation of ([^{Dipp}1]AlOCH$_2$)$_2$: NMR scale: [^{Dipp}**1**]AlH$_2$ (0.010 g, 0.022 mmol) was dissolved in benzene-d_6 (0.5 mL) in an NMR tube fitted with a J. Young's valve and degassed by three freeze-pump-thaw cycles. The tube was pressurised with *ca.* 1 bar of CO_2 at room temperature and the progress of the reaction monitored by ^{1}H NMR spectroscopy. Preparative scale: [^{Dipp}**1**]AlH$_2$ (0.060 g, 0.135 mmol) was dissolved in benzene-d_6 (0.5 mL) in an NMR tube fitted with a J. Young's valve and degassed by three freeze-pump-thaw cycles. The tube was pressurised with *ca.* 1 bar of CO_2 at room temperature and monitored by ^{1}H NMR spectroscopy. When single crystals were yielded from the benzene-d_6 solution, they were analysed by X-ray crystallography and ^{1}H NMR spectroscopy; both sets of data are consistent with those reported in the literature.[21]

[^{Dipp}2]Al(Et){OC(O)H}: [^{Dipp}**2**]Al(Et)H (0.500 g) was dissolved in toluene (15 mL) in an ampoule fitted with a J. Young's valve. The ampoule was attached to a Schlenk line *via* a glass T-piece, the other end of which attached to a 500 mL ampoule filled with *ca.* 1 bar of CO_2, which had been pre-dried over P_2O_5 for 24 h. The solution of [^{Dipp}**2**]Al(Et)H was then degassed by three freeze-pump-thaw cycles and back-filled with the dried CO_2 (*ca.* 1 bar) at room temperature and stirred for 6 h. The solution was subsequently concentrated and stored at −30°C for 3 d, yielding colourless, block-like crystals suitable for X-ray crystallography. Yield: 0.34 g, 62%. ^{1}H NMR (400 MHz, benzene-d_6, 298 K): δ_H –0.24 (2H, q, $^{3}J_{HH}$ = 8.2 Hz, $CH_3C\underline{H}_2Al$), 0.62 (3H, t, $^{3}J_{HH}$ = 8.2 Hz, $C\underline{H}_3CH_2Al$), 1.10 (6H, d, $^{3}J_{HH}$ = 6.8 Hz, CH_3 of Dipp ^{i}Pr), 1.24 (6H, d, $^{3}J_{HH}$ = 6.8 Hz, CH_3 of Dipp ^{i}Pr), 1.27 (6H, d, $^{3}J_{HH}$ = 6.8 Hz, CH_3 of Dipp ^{i}Pr), 1.52 (6H, d, $^{3}J_{HH}$ = 6.8 Hz, CH_3 of Dipp ^{i}Pr), 2.20 (12H, s, CH_3 of NMe_2), 3.01 (2H, sept, $^{3}J_{HH}$ = 6.8 Hz, CH of Dipp ^{i}Pr), 3.84 (1H, s, γ-CH), 3.89 (2H, sept, $^{3}J_{HH}$ = 6.8 Hz, CH of Dipp ^{i}Pr), 7.04 – 7.16 (6H, m, aromatic CH), 8.76 (1H, s, Al{OC(O)H}. ^{13}C{^{1}H} NMR (101 MHz, benzene-d_6, 298 K): δ_C −1.6 (br, $CH_3\underline{C}H_2Al$), 9.0 ($\underline{C}H_3CH_2Al$), 24.4 (CH_3 of Dipp ^{i}Pr), 24.5 (CH_3 of Dipp ^{i}Pr), 26.4 (CH_3 of Dipp ^{i}Pr), 26.6 (CH_3 of Dipp ^{i}Pr), 28.1 (CH of Dipp ^{i}Pr), 28.3 (CH of Dipp ^{i}Pr), 41.2 (CH_3 of NMe_2) 77.3 (γ-CH), 124.6 (*p*-CH of Dipp), 125.2 (*m*-CH of Dipp), 126.3 (*m*-CH of Dipp), 141.5 (*ipso*-C of Dipp), 144.4 (*o*-CH of Dipp), 145.6 (*o*-CH of Dipp), 162.5 (Al{OC(O)H}), 167.5 (NC). ^{27}Al NMR (104 MHz, benzene-d_6, 298 K): δ_{Al} not observed. IR (nujol/cm^{-1}) $\nu_{C=O}$: 1678 (s). Elemental microanalysis: calc. for $C_{34}H_{53}N_4AlO_2$: C 70.80% H 9.26% N 9.71% meas. C 70.58% H 8.98% N 9.51%. Crystallographic data: $C_{34}H_{53}N_4AlO_2$ (M_r = 576.81): monoclinic, *P*2$_1$/*n*, *a* = 11.3065(3), *b* = 23.9993(6), *c* = 12.2822(4) Å, β = 93.483(3) °, *V* = 3326.60(16)) Å^3, *Z* = 4, ρ_c = 1.152 g cm^{-3}, *T* = 150 K, λ = 0.71073 Å, μ(Mo Kα) = 0.096 mm^{-1}, 32606 reflections collected, 9179 independent [R(int) = 0.034] used in all calculations. R_1 = 0.0470, wR_2 = 0.1033 for observed unique reflections [$I > 2\sigma(I)$] and R_1 = 0.0656, wR_2 = 0.1148 for all unique reflections. Max. and min. residual electron densities 0.42, −0.37 e Å^{-3}.

Generation of [^{Dipp}1]Al(Et)(OCH$_2${O(9-BBN)}): Method A: A solution of [^{Dipp}**1**]Al(Et){H$_2$(9-BBN)} (0.018 g, 0.0302 mmol) (prepared from [^{Dipp}**1**]Al(Et)H and 0.5 equiv. of {H(9-BBN)}$_2$) in benzene-d_6 (0.5 mL) in an NMR tube fitted with a J. Young's valve was attached to a Schlenk line *via* a glass T-piece, the other end of which attached to a 500 mL ampoule fitted with a J. Young's valve filled with *ca.* 1 bar of CO_2, pre-dried over P_2O_5 for 24 h. The solution was then degassed by three freeze-pump-thaw cycles and back-filled with dried CO_2 (*ca.* 1 bar) at room temperature and the progress of the reaction monitored by ^{1}H and ^{11}B NMR spectroscopy. Method B: An NMR tube fitted with a J. Young's valve was charged with [^{Dipp}**1**]Al(Et){OC(O)H} (0.020 g, 0.0386 mmol), {H(9-BBN)}$_2$ (0.005 g, 0.0205 mmol) and benzene-d_6 (0.5 mL). The resulting solution was monitored by ^{1}H and ^{11}B NMR spectroscopy. ^{1}H NMR (400 MHz, benzene-d_6, 298 K): δ_H −0.13 (2H, q, $^{3}J_{HH}$ = 8.2 Hz, $CH_3C\underline{H}_2Al$), 0.84 (3H, t, $^{3}J_{HH}$ = 8.2 Hz, $C\underline{H}_3CH_2Al$), 1.08 (6H, d, $^{3}J_{HH}$ = 6.8 Hz, CH_3 of Dipp ^{i}Pr), 1.31 (12H, 2 x overlapping d, $^{3}J_{HH}$ = 6.8 Hz, 2 x CH_3 of Dipp ^{i}Pr), 1.47 (6H, d, $^{3}J_{HH}$ = 6.8 Hz, CH_3 of Dipp ^{i}Pr), 1.59 (6H, s, CH_3 of β-diketiminato backbone), 1.94 (14H, br m, 9-borabicyclo(3.3.1)nonane-CH), 3.21 (2H, sept, $^{3}J_{HH}$ = 6.8 Hz, CH of Dipp ^{i}Pr), 3.76 (2H, sept, $^{3}J_{HH}$ = 6.8 Hz, CH of Dipp ^{i}Pr), 5.02 (1H, s, γ-CH), 5.63 (2H, s, CH_2 of Al-OCH$_2${O(9-BBN)}, 7.09-7.20 (6H, m, aromatic CH). ^{13}C{^{1}H} NMR (101 MHz, benzene-d_6, 298 K): δ_C –2.6 (br, $CH_3\underline{C}H_2Al$), 9.2 ($\underline{C}H_3CH_2Al$), 23.4 (CH_3 of β-

diketiminato backbone), 23.9, 24.5, 24.6, 24.9 (CH_3 of Dipp ^{i}Pr), 25.8 (B-CHCH$_2$C$\underline{H}_2$-), 27.7, 28.9 (CH of Dipp ^{i}Pr), 33.7 (B-CHC$\underline{H}_2$CH$_2$-), 87.6 (CH_2 of Al-OCH$_2${O(9-BBN)}), 99.1 (γ-CH), 124.2, 125.0, 127.4, 141.1, 143.5, 145.4 (ArC of Dipp), 169.9 (NC). Signal for B-$\underline{C}$H not observed. ^{11}B NMR (128 MHz, benzene-d_6, 298 K): δ_B 56.0. ^{27}Al NMR (104 MHz, benzene-d_6, 298 K): δ_{Al} 126.

[^{Dipp}1]Al(Et){O(9-BBN)}: A solution of {H(9-BBN)}$_2$ (0.118 g, 0.482 mmol) in toluene (5 mL) was added at room temperature to a solution of [^{Dipp}**1**]Al(Et){OC(O)H} (0.500 g, 0.964 mmol) (5 mL), with stirring. The reaction mixture was stirred overnight and volatiles were subsequently removed *in vacuo*, yielding a colourless oil. The oil was extracted into minimal diethyl ether, filtered and concentrated to *ca.* 1 mL. Storage of this solution at −30°C for 1 week yielded colourless single crystals suitable for X-ray diffraction. The identity of the crystalline material was shown to be [^{Dipp}**1**]Al(Et){O(9-BBN)} rather than [^{Dipp}**1**]Al(Et)(OCH$_2${O(9-BBN)}). Yield: 0.32 g, 55%. ^{1}H NMR (400 MHz, benzene-d_6, 298 K): δ_H 0.02 (2H, q, $^3J_{HH}$ = 8.1 Hz, CH$_3$C$\underline{H}_2$Al), 1.02 (3H, t, $^3J_{HH}$ = 8.1 Hz, C$\underline{H}_3$CH$_2$Al), 1.10 (6H, d, $^3J_{HH}$ = 6.7 Hz, CH_3 of Dipp ^{i}Pr), 1.24 (6H, d, $^3J_{HH}$ = 6.7 Hz, CH_3 of Dipp ^{i}Pr), 1.30 (6H, d, $^3J_{HH}$ = 6.7 Hz, CH_3 of Dipp ^{i}Pr), 1.42 (6H, d, $^3J_{HH}$ = 6.7 Hz, CH_3 of Dipp ^{i}Pr), 1.53 (6H, s, CH_3 of β-diketiminato backbone), 1.56 (4H, br m, 9-borabicyclo(3.3.1)nonane-CH), 2.04 (10H, br m, 9-borabicyclo(3.3.1)nonane-CH), 3.22 (2H, sept, $^3J_{HH}$ = 6.7 Hz, CH of Dipp ^{i}Pr), 3.55 (2H, sept, $^3J_{HH}$ = 6.7 Hz, CH of Dipp ^{i}Pr), 4.99 (1H, s, γ-CH), 7.07-7.14 (6H, m, aromatic CH). ^{13}C{^{1}H} NMR (101 MHz, benzene-d_6, 298 K): δ_C –1.7 (br, CH$_3$C$\underline{H}_2$Al), 9.2 (C$\underline{H}_3$CH$_2$Al), 23.5 (CH_3 of β-diketiminato backbone), 24.4, 24.7, 24.8, 25.2 (CH_3 of Dipp ^{i}Pr), 25.7 (B-CHCH$_2$C$\underline{H}_2$-), 28.1, 28.5 (CH of Dipp ^{i}Pr), 29.2 (br, B-$\underline{C}$H), 34.6 (B-CH$\underline{C}$H$_2$CH$_2$-), 99.3 (γ-CH), 124.5, 125.0, 127.3, 140.9, 143.7, 145.0 (ArC of Dipp), 170.4 (NC). ^{27}Al NMR (104 MHz, benzene-d_6, 298 K): δ_{Al} not observed. ^{11}B NMR (128 MHz, benzene-d_6, 298 K): δ_B 55.0. EI-MS: *m/z* calc for $C_{31}H_{46}N_2Al$–([M{O(9-BBN)}]$^+$) 473.3476, meas. 473.3457 (3%), calc. for $C_{37}H_{55}N_2AlBO$ ([M–Et]$^+$) 581.4223, meas. 581.4216 (5%). Crystallographic data: $C_{39}H_{60}N_2AlBO$ (M_r = 610.71): monoclinic, $P2_1/n$, a = 9.4149(2), b = 18.1696(4), c = 21.4970(4) Å, β = 91.3346(18) °, V = 3676.39(13) Å^3, Z = 4, ρ_c = 1.103 g cm^{-3}, T = 150 K, λ = 1.54184 Å, μ(Cu Kα) = 0.703 mm^{-1}, 37421 reflections collected, 7614 independent [R(int) = 0.031] used in all calculations. R_1 = 0.0487, wR_2 = 0.1275 for observed unique reflections [$I > 2\sigma(I)$] and R_1 = 0.0503, wR_2 = 0.1299 for all unique reflections. Max. and min. residual electron densities 0.86, −0.83 e Å^{-3}.

[^{Dipp}1]Al(Et)(OB(H)OMe): [^{Dipp}**1**]Al(Et){OC(O)H} (0.300 g, 0.579 mmol) was dissolved in toluene (5 mL) and BH_3·SMe_2 (165 μL, 1.74 mmol) added. The reaction mixture was stirred overnight at room temperature, followed by the removal of volatiles *in vacuo*, yielding a sticky, colouress oil. The oil was dissolved in *n*-hexane (*ca*. 2 mL), filtered (leaving behind a white residue) and concentrated until the point of incipient crystalisation. The solution was stored at 6°C for several hours, yielding colourless rod-shaped crystals, suitable for X-ray diffraction. Yield: 0.13 g, 41%. ^{1}H{^{11}B} NMR (400 MHz, benzene-d_6, 298 K): δ_H −0.12 (2H, q, $^3J_{HH}$ = 8.1 Hz, CH$_3$C$\underline{H}_2$Al), 0.83 (3H, t, $^3J_{HH}$ = 8.1 Hz, C$\underline{H}_3$CH$_2$Al), 1.05 (6H, d, $^3J_{HH}$ = 6.8 Hz, CH_3 of Dipp ^{i}Pr), 1.23 (6H, d, $^3J_{HH}$ = 6.8 Hz, CH_3 of Dipp ^{i}Pr), 1.32 (6H, d, $^3J_{HH}$ = 6.8 Hz, CH_3 of Dipp ^{i}Pr), 1.38 (6H, d, $^3J_{HH}$ = 6.8 Hz, CH_3 of Dipp ^{i}Pr), 1.55 (6H, s, CH_3 of β-diketiminato backbone), 3.22 (2H, sept, $^3J_{HH}$ = 6.8 Hz, CH of Dipp ^{i}Pr), 3.57 (2H, sept, $^3J_{HH}$ = 6.8 Hz, CH of Dipp ^{i}Pr), 3.63 (3H, s, CH_3 of B-OMe), 4.77 (1H, br s, BH), 4.96 (1H, s, γ-CH), 7.07-7.16 (6H, m, aromatic CH), ^{13}C{^{1}H} NMR (101 MHz, benzene-d_6, 298 K): δ_C −2.2 (br, CH$_3$C$\underline{H}_2$Al), 9.0 (C$\underline{H}_3$CH$_2$Al), 23.3 (CH of Dipp ^{i}Pr) 24.2, 24.3, 24.9, 26.3 (CH_3 of Dipp ^{i}Pr), 27.7, 29.0 (CH of Dipp ^{i}Pr), 50.0 (CH_3 of BOMe), 98.3 (γ-CH), 124.1, 125.0, 127.5, 140.6, 143.4, 145.3 (ArC of Dipp), 170 (NC). ^{11}B{^{1}H} NMR (128 MHz, benzene-d_6, 298 K): δ_B 25.1 (s, $\Delta\omega_{1/2}$ = 458 Hz ^{1}H decoupled, $\Delta\omega_{1/2}$ = 1102 Hz ^{1}H coupled). ^{27}Al NMR (104 MHz, benzene-d_6, 298 K): δ_{Al} not observed. EI-MS: *m/z* calc for $C_{30}H_{45}N_2AlBO_2$ ([M–Et]$^+$) 503.3389, meas. 503.3400 (100%), calc for $C_{32}H_{51}N_2AlBO_2$ ([M+H]$^+$) 533.3859, meas. 533.3517 (10%) IR (nujol/cm^{-1}) ν_{B-H} : 2434 (w). Crystallographic data: $C_{32}H_{50}N_2AlBO_2$ (M_r = 532.53): monoclinic, $P2_1/c$, a = 21.2295(5), b = 9.3528(2), c = 17.6803(4) Å, β = 111.721(3) °, V = 3261.26(14) Å^3, Z = 4, ρ_c = 1.085 g cm^{-3}, T = 150 K, μ(Cu Kα) = 0.751 mm^{-1}, λ = 1.54180 Å. 17768 reflections collected, 6726 independent [R(int) = 0.0487] used in all calculations. R_1 = 0.0536, wR_2 = 0.1405 for observed unique reflections [$I > 2\sigma(I)$] and R_1 = 0.0684, wR_2 = 0.1591 for all unique reflections. Max. and min. residual electron densities 0.369, −0.384 e Å^{-3}.

Acknowledgements

We acknowledge funding from EPSRC (AC studentship), Oxford-SCG Centre of Excellence (JH), EU Marie Curie program (ELK, grant number PIEF-GA-2013-626441). We thank Drs M. Ángeles Fuentes, Rémi Tirfoin and Jesús Campos for additional crystallographic input.

Keywords: aluminium • hydride • carbon dioxide • reduction • β-diketiminate

[1] K. Huang, C.-L. Sun, Z.-J. Shi, *Chem. Soc. Rev.* **2011**, *40*, 2435-2452.
[2] J. Schneider, H. Jia, J.T. Muckerman, E. Fujita, *Chem. Soc. Rev.* **2012**, *41*, 2036–2051.
[3] Q. Liu, L. Wu, R. Jackstell, M. Beller, *Nature Commun.* **2015**, *6*, 5933-5948.
[4] L.J. Murphy, K.N. Robertson, R.A. Kemp, H.M. Tuononen, J.A.C. Clyburne, *Chem. Commun.* **2015**, *51*, 3942–3956.
[5] A. Tlili, E. Blondiaux, X. Frogneux, T. Cantat, *Green Chem.* **2015**, *17*, 157–168.
[6] S. Chakraborty, J. Zhang, J.A. Krause, H. Guan, *J. Am. Chem. Soc.* **2010**, *132*, 8872–8873.
[7] S. Chakraborty, J. Zhang, Y.J. Patel, J.A. Krause, H. Guan, *Inorg. Chem.* **2013**, *52*, 37–47.
[8] R. Shintani, K. Nozaki, *Organometallics* **2013**, *32*, 2459–2462.
[9] H.-W. Suh, L.M. Guard, N. Hazari, *Chem. Sci.* **2014**, *5*, 3859-3872.
[10] A. Berkefeld, W.E. Piers, M. Parvez, L. Castro, L. Maron, O. Eisenstein, *Chem. Sci.* **2013**, *4*, 2152-2162.
[11] S. Bontemps, L. Vendier, S. Sabo-Etienne, *J. Am. Chem. Soc.* **2014**, *136*, 4419–4425.

[12] S. Bontemps, L. Vendier, S. Sabo-Etienne, *Angew. Chem. Int. Ed.* **2012**, *51*, 1671–1674.

[13] G. Jin, C.G. Werncke, Y. Escudié, S. Sabo-Etienne, S.J. Bontemps, *J. Am. Chem. Soc.* **2015**, *137*, 9563–9566.

[14] S. Bontemps, S. Sabo-Etienne, *Angew. Chem. Int. Ed.* **2013**, *52*, 10253–10255.

[15] F. Huang, C. Zhang, J. Jiang, Z.X. Wang, H. Guan, *Inorg. Chem.* **2011**, *50*, 3816–3825.

[16] M.D. Anker, M. Arrowsmith, P. Bellham, M.S. Hill, G. Kociok-Köhn, D.J. Liptrot, M.F. Mahon, C. Weetman, *Chem. Sci.* **2014**, *5*, 2826-2830.

[17] D. Mukherjee, S. Shirase, T.P. Spaniol, K. Mashima, J. Okuda, *Chem. Commun.* **2016**, *52*, 13155–13158.

[18] D. Mukherjee, H. Osseili, T.P. Spaniol, J. Okuda, *J. Am. Chem. Soc.* **2016**, *138*, 10790–10793.

[19] A. Jana, D. Ghoshal, H.W. Roesky, I. Objartel, G. Schwab, D. Stalke, *J. Am. Chem. Soc.* **2009**, *131*, 1288–1293.

[20] A. Jana, H.W. Roesky, C. Schulzke, A. Döring, *Angew. Chem. Int. Ed.* **2009**, *48*, 1106–1109.

[21] G. Tan, W. Wang, B. Blom, M. Driess, *Dalton Trans.* **2014**, *43*, 6006–6011.

[22] T.J. Hadlington, C.E. Kefalidis, L. Maron, C. Jones, *ACS Catal.* **2017**, *7*, 1853-1859.

[23] J.A.B. Abdalla, I.M. Riddlestone, R. Tirfoin, S.Aldridge, *Angew. Chem. Int. Ed.* **2015**, *54*, 5098–5102.

[24] A. Jana, G. Tavčar, H.W. Roesky, M. John, *Dalton Trans.* **2010**, *39*, 9487–9489.

[25] S. Aldridge, A.J. Downs, *Chem. Rev.* **2001**, *102*, 3305-3366

[26] P.C. Kuo, I.C. Chen, J.C. Chang, M.T. Lee, C.H. Hu, C. Hung, H.M. Lee, J.H. Huang, *Eur. J. Inorg. Chem.* **2004**, 4898–4906.

[27] T.W. Myers, L.A. Berben, *Chem. Sci.* **2014**, *5*, 2771-2777.

[28] A.E. Finholt, E.C. Jacobson, *J. Am. Chem. Soc.* **1952**, *74*, 3943–3944.

[29] Z. Yang, M. Zhong, X. Ma, K. Nijesh, S. De, P. Parameswaran, H.W. Roesky, *J. Am. Chem. Soc.* **2016**, *138*, 2548–2551.

[30] A. Bismuto, S.P. Thomas, M.J. Cowley, *Angew. Chem. Int. Ed.* **2016**, *55*, 15356–15359.

[31] A. Bismuto, M.J. Cowley, S.P. Thomas, *ACS Catal.* **2018**, *8*, 2001–2005.

[32] D. Franz, L. Sirtl, A. Pöthig, S. Inoue, *Z. Anorg. Allg. Chem.* **2016**, *642*, 1245–1250.

[33] K. Jakobsson, T. Chu, G.I. Nikonov, *ACS Catal.* **2016**, *6*, 7350–7356.

[34] Z. Yang, M. Zhong, X. Ma, S. De, C. Anusha, P. Parameswaran, H.W. Roesky, *Angew. Chem. Int. Ed.* **2015**, *54*, 10225–10229.

[35] V.K. Jakhar, M.K. Barman, S. Nembenna, *Org. Lett.* **2016**, *18*, 4710–4713.

[36] V.A. Pollard, S.A. Orr, R. McLellan, A.R. Kennedy, E. Hevia, R.E. Mulvey, *Chem. Commun.* **2018**, *54*, 1233–1236.

[37] Aluminium complexes have been used in catalytic CO_2 reduction processes as the Lewis acidic component of a frustrated Lewis pair: a) G. Ménard, D.W. Stephan, *J. Am. Chem. Soc.* **2010**, *132*, 1796–1797; b) G. Ménard, D.W. Stephan, *Angew. Chem. Int. Ed.* **2011**, *50*, 8396–8399; c) J. Boudreau, M.-A. Courtemanche, F.-G. Fontaine, *Chem. Commun.* **2011**, *47*, 11131-11133; d) G. Ménard, D.W. Stephan, *Dalton Trans.* **2013**, *42*, 5447-5453; e) M.-A. Courtemanche, J. Larouche, M.-A. Légaré, W. Bi, L. Maron, F.-G. Fontaine, *Organometallics* **2013**, *32*, 6804–6811.

[38] C. Cui, H.W. Roesky, H. Hao, H.G. Schmidt, M. Noltemeyer, *Angew. Chem. Int. Ed.* **2000**, *39*, 1815–1817.

[39] D.C.H. Do, A. Keyser, A.V. Protchenko, B. Maitland, I. Pernik, H. Niu, E. Kolychev, A. Rit, D. Vidovic, A. Stasch, C. Jones, S. Aldridge, *Chem.-Eur. J.* **2017**, *23*, 5830-5841.

[40] B. Twamley, N.J. Hardman, P.P. Power, *Acta Crystallogr. E* **2001**, *57*, m227–m228.

[41] S. Singh, H.-J. Ahn, A. Stasch, V. Jancik, H.W. Roesky, A. Pal, M. Biadene, R. Herbst-Irmer, M. Noltemeyer, H.-G. Schmidt, *Inorg. Chem.* **2006**, *45*, 1853–1860.

[42] M. Stender, B.E. Eichler, N.J. Hardman, P.P. Power, J. Prust, M. Noltemeyer, H.W. Roesky, *Inorg. Chem.* **2001**, *40*, 2794-2799.

[43] T. Chu, I. Korobkov, G.I. Nikonov, *J. Am. Chem. Soc.* **2014**, *136*, 9195–9202.

[44] R.M. Badger, *J. Chem. Phys.* **1934**, *2*, 128–131.

[45] K. Ziegler, F. Krupp, K. Weyer, W. Larbig, *Justus Liebigs Ann. Chem.* **1960**, *629*, 251–256

[46] C.C. Chong, R. Kinjo, *ACS Catal.* **2015**, *5*, 3238–3259.

[47] S. Pereira, M. Srebnik, *Organometallics* **1995**, *14*, 3127–3128.

[48] A.W. Kyri, R. Kunzmann, G. Schnakenburg, Z.-W. Qu, S. Grimme, R. Streubel, *Chem. Commun.* **2016**, *52*, 13361–13364.

[49] G.W. Kramer, H.C. Brown, *J. Organomet. Chem.* **1974**, *73*, 1–15.

[50] R. Köster,Y.-H. Tsay, C. Krüger, J. Serwatowski, *Chem. Ber.* **1986**, *119*, 1174–1188.

[51] C. Das Neves Gomes, E. Blondiaux, P. Thuéry, T. Cantat, *Chem.-Eur. J.* **2014**, *20*, 7098–7106.

[52] *Boron Reagents in Synthesis* (Ed.: A. Coca), ACS Symposium Series, American Chemical Society, Washington, **2016**, Vol. 1236.

[53] M.-A. Courtemanche, M.-A.; Légaré, L. Maron, F.G. Fontaine, *J. Am. Chem. Soc.* **2014**, *136*, 10708–10717.

[54] M.-A. Courtemanche, M.-A.; Légaré, L. Maron, F.G. Fontaine, *J. Am. Chem. Soc.* **2013**, *135*, 9326–9329.

[55] G. Glockler, *Trans. Faraday Soc.* **1963**, *59*, 1080-1085.

[56] M. Diem, in *Modern Vibrational Spectroscopy and Micro-Spectroscopy*, Wiley, Chichester, **2015**, 397–398.

[57] A.J. Downs, H.-J. Himmel in *The Group 13 Metals Aluminium, Gallium, Indium and Thallium; Chemical Patterns and Peculiarities* (Eds.: S. Aldridge, A.J. Downs) Wiley, Chichester, UK.

[58] Y. Yang, P.M. Prabhuodeyara, H. Ye, Z. Zhang, H.W. Roesky, P.W. Jones, *J. Organomet. Chem.* **2008**, *693*, 1455-1461.

[59] J.K. Ruff, M.F. Hawthorne, *J. Am. Chem. Soc.* **1961**, *82*, 2141-2144.

[60] crystallography refs

Entry for the Table of Contents (Please choose one layout)

FULL PAPER

Al-O, Al-O, Al-O

Mononuclear β-diketiminate stabilized hydrides have recently been implicated in a number of reduction processes of C=O bonds. Here we show that turnover in the borane reduction of CO_2 by a range of such complexes is rendered thermodynamically non-viable by the excessive strength of the Al-O bond.

((Insert TOC Graphic here: max. width: 5.5 cm; max. height: 5.0 cm))

Alexa Caise, Dafydd Jones, Eugene L. Kolychev, Jamie Hicks, Jose M. Goicoechea and Simon Aldridge**

Page No. – Page No.

On the viability of catalytic turnover via Al-O/B-H metathesis: the reactivity of β-diketiminate aluminium hydrides towards CO_2 and boranes